




Redox Zone and Trophic State as Drivers of Methane-Oxidizing Bacterial Abundance and Community Structure in Lake Sediments

Journal Article**Author(s):**

van Grinsven, Sigrid; [Meier, Dimitri](#) ; Michel, Anja; Han, Xingguo; [Schubert, Carsten](#) ; [Lever, Mark](#) 

Publication date:

2022-03

Permanent link:

<https://doi.org/10.3929/ethz-b-000536706>

Rights / license:

[Creative Commons Attribution 4.0 International](#)

Originally published in:

Frontiers in Environmental Science 10, <https://doi.org/10.3389/fenvs.2022.857358>

Funding acknowledgement:

163371 - Role of Bioturbation in Controlling Microbial Community Composition and Biogeochemical Cycles in Marine and Lacustrine Sediments (SNF)



Redox Zone and Trophic State as Drivers of Methane-Oxidizing Bacterial Abundance and Community Structure in Lake Sediments

OPEN ACCESS

Edited by:

Yves T Prairie,
Université du Québec à Montréal,
Canada

Reviewed by:

Nils Risgaard-Petersen,
Aarhus University, Denmark
Dirk de Beer,
Max Planck Society, Germany

***Correspondence:**

Sigrid van Grinsven
sigrid.vangrinsven@eawag.ch
Mark A. Lever
mark.lever@usys.ethz.ch

†Present address:

Xingguo Han,
Federal Institute for Forest, Snow, and
Landscape Research (WSL),
Zürcherstrasse, Switzerland

†These authors have contributed
equally to this work and share first
authorship

Specialty section:

This article was submitted to
Biogeochemical Dynamics,
a section of the journal
Frontiers in Environmental Science

Received: 18 January 2022

Accepted: 14 February 2022

Published: 10 March 2022

Citation:

van Grinsven S, Meier DV, Michel A,
Han X, Schubert CJ and Lever MA
(2022) Redox Zone and Trophic State
as Drivers of Methane-Oxidizing
Bacterial Abundance and Community
Structure in Lake Sediments.
Front. Environ. Sci. 10:857358.
doi: 10.3389/fenvs.2022.857358

**Sigrid van Grinsven^{1*†}, Dimitri V. Meier^{2†}, Anja Michel², Xingguo Han^{2†},
Carsten J. Schubert^{1,2} and Mark A. Lever^{2*}**

¹Eawag, Swiss Federal Institute of Aquatic Science and Technology, Department of Surface Waters, Research and Management, Kastanienbaum, Switzerland, ²Institute of Biogeochemistry and Pollutant Dynamics, Swiss Federal Institute of Technology, Zurich, Switzerland

Eutrophication is expected to increase methane production in freshwater sediments worldwide over the coming decades. Methane-oxidizing bacteria (MOB) consume a significant fraction of this sedimentary methane, but the factors that control their distributions and activities are not understood. By combining genetic approaches (*pmoA*, 16S rRNA gene, metagenomics) with geochemical and sedimentological analyses, we investigate the role of trophic state, electron acceptors, oxygen (O₂) and methane fluxes, and potential methylotrophic partner organisms in driving the distributions, abundances, and community compositions of MOB across five lakes in central Switzerland. Although methane fluxes were highest in the eutrophic lakes, methanotrophic abundances peaked in oxic and anoxic sediments of an oligotrophic lake. In all lakes, Type I gammaproteobacterial Methylococcaceae dominated oxic and suboxic bottom water and surface sediments, showing strong correlations with abundances of putatively methylotrophic Methylophilaceae, whereas Type II alphaproteobacterial Methylocystaceae increased in deeper, anoxic sediment layers. Methanotrophic bacteria belonging to the NC10 phylum were predominantly detected within denitrifying sediment of the oligotrophic lake, matching their presumed nitrite-dependent lifestyle. While dominant MOB taxa at the genus-level follow vertical distributions of different aerobic and anaerobic respiration reactions, trophic state at the time of sediment deposition was the best predictor of MOB community structure at the operational taxonomic unit (OTU) level. Elevated methane fluxes combined with low MOB abundances in surface sediments of eutrophic lakes, moreover, support the notion that in eutrophic lakes a major portion of sedimentary methane bypasses the biological methane filter and escapes to overlying water.

Keywords: greenhouse gas emissions, MOB, methanotrophy, microbial community, eutrophication, oligotrophic, methane oxidation, *pmoA*

INTRODUCTION

Freshwater lakes account for 6–16% of natural emissions of the greenhouse gas methane (CH₄) to the atmosphere (Bastviken et al., 2004). Most of this methane is biologically produced in lake sediments. A fraction of this biologically produced methane escapes into the water column by diffusion, ebullition, and advective processes, and is subsequently emitted to the atmosphere (Tranvik et al., 2009; Bastviken et al., 2011; Dean et al., 2018). Methane emissions from lakes to the atmosphere are predicted to increase due to global temperature increases over the coming decades (Dean et al., 2018; Guo et al., 2020; Zhu et al., 2020).

Besides warming, anthropogenic increases in nutrient inputs that enhance primary production and organic carbon loading (eutrophication), can increase methane emissions from lakes (Beaulieu et al., 2019). Hereby enhanced supplies of algal organic carbon stimulate organic matter (OM) mineralization rates and lead to higher respiration rates of the electron acceptors dioxygen (O₂), nitrate (NO₃⁻), sulfate (SO₄²⁻), and metal oxides (Fe(III), Mn(IV)) in lake water and surface sediment. The more rapid depletion of these electron acceptors in lake sediments, combined with the higher OM availability, promotes microbial methane production (methanogenesis) (Fiskal et al., 2019) and results in increased sedimentary methane release under eutrophic conditions (Beaulieu et al., 2019; Sanches et al., 2019).

Most microbially produced methane in lake sediments is microbially oxidized in surface sediments before it can escape to the overlying water. Methane oxidation removes from ~50 to 99% of sedimentary methane, with removal efficiencies being highest in oligotrophic and lowest in eutrophic lakes (D'Ambrosio and Harrison, 2021). Previously, it was believed that lake sedimentary methanotrophy was performed exclusively by aerobic methane-oxidizing bacteria (MOB) within the Alpha- and Gammaproteobacteria (e.g., Auman et al., 2000; Frenzel et al., 1990; Pester et al., 2011; Reim et al., 2012; reviewed in; Knief, 2015). Since then it was shown that Bacteria of the genus *Methylomirabilis* (phylum: NC10) perform anaerobic methane oxidation coupled to nitrite (NO₂⁻) reduction (denitrification; Ettwig et al., 2010; Deutzmann et al., 2014), while Archaea of the family Methanoperedenaceae (phylum: Euryarchaeota) couple the anaerobic oxidation of methane to the reduction of NO₃⁻, Mn(IV) or Fe(III) (Ettwig et al., 2016; Leu et al., 2020).

Although historically considered to be obligately aerobic, MOB are widespread in O₂-depleted sediments, and in some cases even reach their highest gene copy numbers in anoxic subsurface layers (Rahalkar et al., 2009; Pester et al., 2011; Tsutsumi et al., 2011; He et al., 2021; Lyautey et al., 2021). Recently, members of the gammaproteobacterial genera *Methylobacter* and *Methylomonas* were shown to oxidize methane syntrophically with denitrifying methylotrophic Betaproteobacteria (Methylophilaceae). Hereby the MOB partially oxidize methane to methanol, H₂, or short-chain organic acids (e.g., formate, acetate), which the partner organisms subsequently oxidize to gain energy by denitrification (Beck et al., 2013; Kalyuzhnaya et al., 2013; Oshkin et al., 2014). In addition, several gammaproteobacterial

genera (e.g., *Methylomonas*, *Methylobacter*, *Methylomicrobium*) have been shown to directly couple methane oxidation to denitrification under O₂-limiting conditions (Kits et al., 2015b; Cao et al., 2019; van Grinsven et al., 2020a). Recently, stimulation of bacterial methane oxidation rates by iron (III), manganese (IV), and humic compounds has been shown (Oswald et al., 2016; He et al., 2021; van Grinsven et al., 2021) and that certain strains of *Methylomonas* (Gammaproteobacteria) and *Methylosinus* (Alphaproteobacteria) can use ferrihydrite minerals as electron acceptors to oxidize methane (Zheng et al., 2020).

The community composition of MOB in lake sediments has so far mainly been studied by microbial enrichment and isolation methods (e.g., Auman et al., 2000; He et al., 2012; Danilova et al., 2016), and by cultivation-independent methods involving fluorescence-in-situ-hybridization (FISH; Rahalkar et al., 2009), sequencing of 16S rRNA genes (Fiskal et al., 2021; Pierangeli et al., 2021), and sequencing of catabolic functional genes (for reviews see (McDonald et al., 2008; Knief, 2015). Hereby *pmoA*, a functional gene that encodes the catalytic subunit of particulate methane monooxygenase (pMMO), an enzyme which performs the initial conversion of methane to methanol, has been widely targeted. The reasons are that *pmoA* is present in almost all known MOB (exception: Beijerinckiaceae), *pmoA*-based phylogenies agree largely with 16S rRNA gene-based phylogenies, and *pmoA* is sufficiently conserved to be suitable for polymerase chain reaction (PCR)-based quantification and sequencing methods.

Even though these methods have greatly advanced knowledge on the distributions of MOB in lake sediments, major knowledge gaps remain. A crucial knowledge gap concerns how increases in sedimentary methane production due to eutrophication and in response to warming impact the activity and community structure of MOB. Moreover, while changes in MOB community structure across oxic-anoxic interfaces are well-studied, little is known about MOB distributions in relation to anaerobic electron acceptors in deeper layers, where MOB often remain abundant. Vertical distributions of these electron acceptors in sediments could shape niches of MOB in ways similar to stratified eutrophic lakes, in which vertical zonations of MOB along redox and methane gradients have been documented (Mayr et al., 2020).

Here we investigate the influence of eutrophication and electron acceptor gradients on the activity, abundance, and community structure of MOB by analyzing sediment cores from five lakes in central Switzerland. These lakes have well-documented trophic histories and today range from oligotrophic (Lake Lucerne) to mesotrophic (Lake Zurich) to eutrophic (Lake Zug, Lake Baldegg, Lake Greifen) (Fiskal et al., 2019). By analyzing sedimentary records that span the entire history of anthropogenic eutrophication starting in the late 19th and early 20th century, we examine if (past) changes in lake trophic state are reflected in MOB community structure at the genus- and operational taxonomic unit (OTU)-level based on *pmoA* sequences today. Based on *pmoA* copy numbers as a proxy for MOB abundance and diffusive fluxes of O₂ and methane in surficial sediment, we investigate whether methane or O₂ availability are key drivers of MOB community size. Using

TABLE 1 | Depth intervals (in cm) of respiration reactions (average \pm standard deviation of three stations) across the five lakes (based on **Figure 5** in Fiskal et al., 2019).

	Lake greifen (eutrophic)	Lake baldegg (eutrophic)	Lake zug (eutrophic)	Lake zurich (mesotrophic)	Lake lucerne (oligotrophic)
Aerobic	0–0.17 \pm 0.03	0–0.08 \pm 0.02	0–0.23 \pm 0.03	0–0.22 \pm 0.08	0–0.73 \pm 0.25
Denitrification	0–2.5 \pm 1.0	0–2.8 \pm 1.2	0–7.7 \pm 3.1	0–3.3 \pm 1.4	0–9.0 \pm 2.0
Sulfate reduction	0–5.8 \pm 2.0	0–6.2 \pm 3.3	0–11.7 \pm 3.1	0–10.3 \pm 1.2	0–11.0 \pm 2.0
Mn(IV) reduction	0.3 \pm 0.3–8.2 \pm 4.9	0.3 \pm 0.3–14 \pm 7	0.5 \pm 0.0–5.0 \pm 0.0	0.3 \pm 0.3–24 \pm 15	0.7 \pm 0.8–bottom
Fe(III) reduction	0.5 \pm 0.0–bottom	throughout	0.5 \pm 0.0–bottom	0.5 \pm 0.0–bottom	0.8 \pm 0.6–bottom
Methanogenesis	throughout	throughout	throughout	2.6 \pm 2.4–bottom	3.0 \pm 1.7–bottom

published vertical distributions of respiration reactions (Fiskal et al., 2019), we examine relationships between *in situ* distributions of respiration reactions and MOB abundances and community structure. Finally, we explore the influence of (past) trophic state and dominant respiration reactions on syntrophic partnerships of MOB and methylotrophic partner organisms based on correlations between MOB genera and OTUs from this study and published 16S rRNA gene sequences of methylotrophic bacteria from Han et al. (2020). Our results provide key insights into how eutrophication history and present-day electron acceptor distributions interact to control the community structure and activity of MOB in lake sediments.

MATERIALS AND METHODS

Site Descriptions and Lake Trophic Histories

This study is part of the larger research effort “Lake Eutrophication Impacts on Carbon Accumulations in Sediments” (LEICAS), in which the long-term consequences of eutrophication on sediment biogeochemistry, microbiology, and ecosystem ecology are investigated. LEICAS was initiated in 2016, when Lake Lucerne, Lake Zurich, Lake Zug, Lake Baldegg, and Lake Greifen were each sampled at three stations that covered a water depth gradient from shallow sublittoral to profundal sediments. Biogeochemical, organic geochemical, and 16S rRNA gene-based microbiological data on all stations were published previously by Fiskal et al. (2019, 2021a) and Han et al. (2020). An experimental study to investigate impacts of lake “oligotrophication” on sedimentary processes has also been published (Fiskal et al. 2021b). Depth profiles of respiration zones are summarized in **Table 1**.

The five lakes all experience seasonal changes in primary production, thermal stratification, and sedimentation (Teranes et al., 1999; Bürgi, 2000; Naeher et al., 2013), but differ in land use and anthropogenic eutrophication histories (Fiskal et al., 2019). Despite minor increases in total P concentrations in the 1960s and 1970s, Lake Lucerne has always remained oligotrophic. Lake Zurich became eutrophic, as evidenced by the development of permanently hypoxic conditions in its deep basin, around 1890 (Naeher et al., 2013), but has been mesotrophic since ~1980 due to

improved wastewater management. The three eutrophic lakes became eutrophic at different times (Lake Baldegg: ~1870; Lake Greifen: ~1920; Lake Zug: ~1930) and have remained eutrophic since. The high rates of primary production in Lake Greifen, Lake Baldegg, and Lake Zug are sustained by the retention and recycling of P that was introduced in the 20th century. Despite artificial water column mixing and aeration (Lake Baldegg: since 1982/83; Lake Greifen: since 2009), Lake Baldegg experiences strong decreases in O₂ concentrations over the summer months, and Lake Greifen continues to develop seasonal hypoxia or anoxia below 10 m water depth from June–December (for details see Supplement of Fiskal et al., 2019, and references therein).

Sample Collection

In June and July 2016, three stations that differed in water depth were sampled in each lake (Lake Lucerne: 15, 24, 32 m; Lake Zurich: 25, 45, 137 m; Lake Zug: 25, 35, 50 m; Lake Baldegg: 21, 45, 66 m; Lake Greifen: 15, 24, 32 m) using 15-cm diameter gravity cores (UWITEC, AT). Bottom water temperatures at the time of sampling were 6–7°C at all stations except the shallow (9°C) and deep stations (5°C) in Lake Lucerne. All sites were bioturbated and contained benthic infaunal chironomids and/or oligochaetes (Fiskal et al., 2021a), except the deep, permanently hypoxic station in Lake Zurich. Sediment porewater for downstream measurements of dissolved electron acceptors (nitrate, sulfate, dissolved inorganic carbon) and respiration end products (Mn²⁺, Fe²⁺, ammonium) was sampled using rhizons (0.2 μ m pore size, Rhizosphere) from a designated core with pre-drilled holes that were taped prior to coring. Solid-phase sediment samples for cell counts, DNA analyses, methane and total organic carbon (TOC) quantifications, and physical property determinations (porosity, density) were taken from an additional core using sterile cut-off syringes. Porewater cores were sampled in 1-cm depth intervals from 0–4 cm, 2-cm intervals from 4–20 cm, and 4-cm intervals from 36–40 cm. The same sampling resolution was applied during solid-phase sediment sampling, except that the top 0–2 cm were sampled at enhanced resolution (0.5 cm depth intervals). For further details on all sampling procedures, see Fiskal et al. (2019).

Additional cores were taken at each station for the measurement of O₂ concentration profiles in surface sediments using Clark-type microsensors (Unisense A/S, DK), macrofaunal

TABLE 2 | *pmoA* primers used in this study.

(A)		
<i>pmoA</i> primer name	Primer sequence (5'-3')	References
<i>pmoA</i> A189F	GGN GAC TGG GAC TTC TGG	Holmes et al. (1995)
<i>pmoA</i> _Mb661R	CCG GMG CAA CGT CYT TAC C	Costello and Lidstrom, (1999)
NC10- <i>pmoA</i> 239F	GTT GAC GCC GAT CCT GTT	This study
NC10- <i>pmoA</i> 590 R	GCA CAT ACC CAT CCC CAT	This study

(B)		
	Time (min:s)	Temperature (°C)
1. Initial Activation	5:00	95
2. Denaturation	0:15	95
3. Annealing	0:30	62 → 53
4. Elongation	0:30	72
<i>Steps 2–4 repeated 10x</i>		
5. Denaturation	0:15	95
6. Annealing	0:30	52
7. Elongation	0:30	72
8. Acquisition	0:05	85
<i>Steps 5–8 repeated 35x</i>		
6. Denaturation	1:15	95
7. Acquisition	continuous	55–95
8. Cooling	∞	4

(C)		
	Time (min:s)	Temperature (°C)
1. Initial Activation	5:00	95
2. Denaturation	0:45	95
3. Annealing	0:30	62
4. Elongation	1:00	72
<i>Steps 2–4 repeated 30–50x</i>		
6. Final elongation	5:00	72
8. Cooling	∞	4

(A) *pmoA* primers used in this study. (B) Protocol for qPCR amplification using general *pmoA* primer pair (A189F–Mb661R). During the initial 10 cycles a touch-down PCR was used, during which the annealing temperature decreased in 1°C intervals. The same protocol was used for the NC10-*pmoA*29F/NC10-*pmoA*590R primer combination except that the annealing temperature was maintained at 62°C. (C) PCR amplification protocols for sequencing. The same protocol was used for both primer combinations.

community analyses, and sedimentological analyses (including Cs-137 and unsupported Pb-210 for sediment dating; further details and data in Fiskal et al. (2019, 2021a)).

Geochemical Analyses

O₂ and methane concentration profiles were published previously by Fiskal et al. (2019). Vertical concentration profiles of O₂ were measured using Clark-type microsensors (Unisense A/S) while methane concentrations were measured by gas chromatography using a flame-ionization detector (for details see Fiskal et al. (2019)). Vertical distributions of respiration reactions, based on porewater-dissolved concentrations of O₂, nitrate, sulfate, Mn²⁺, Fe²⁺ and CH₄, were also determined in Fiskal et al. (2019).

DNA Extraction

DNA was extracted from all solid-phase samples according to Lever et al. (2015). Sediments from Lake Zug, Lake Zurich and Lake Lucerne were extracted according to lysis protocol II. Due to high humic acid concentrations that interfered with post-extraction column-based DNA purification, sediments from Lake Greifen and Lake Baldeg were treated with an additional

humic acid removal step prior to purification (lysis protocol III). For detailed protocols, see Han et al. (2020).

Quantification and Sequencing of *pmoA* Genes

pmoA was PCR-amplified using the general A189F - Mb661R *pmoA* primer combination (Holmes et al., 1995; Costello and Lidstrom, 1999) and the new NC10-*pmoA*239F–NC10-*pmoA*590R primer pair (Table 2A). The latter primer pair was specifically designed to amplify *pmoA* sequences of denitrifying methane-oxidizing *Methylomirabilales*, which are not amplified using the general primer pair but were detected in 16S rRNA gene libraries of the five lakes (Han et al., 2020). The general A189F - Mb661R combination was used both for quantitative PCR (qPCR), using complete *pmoA* gene sequences of *Methylococcus capsulatus* as qPCR standards, and for Illumina MiSeq-based community analyses.

For each of the 15 stations, qPCR analyses and sequencing were performed on 7 to 10 samples (Supplementary Table S1). Key sample targets included bottom water, sediments above and right below the oxic-anoxic transition in the upper few centimeters, samples from anoxic layers with denitrification and sulfate

reduction (typically to ≤ 10 cm), and samples from deeper layers where methanogenesis, iron (III) and manganese (IV) reduction were the only detectable respiration reactions (**Table 1**). qPCR was done with SYBR Green I Master Mix on a LightCycler 480 II (Roche Molecular Systems). Each 10- μ L reaction mixture consisted of 5 μ L Roche Light Cycler Master Mix containing SYBRTM Green, 0.5 μ L of each 50 μ M primer solution, 1 μ L of 1 mg ml⁻¹ bovine serum albumin, 2 μ L of DNA extract, and 1 μ L of molecular-grade water (for qPCR cyclor protocol see **Table 2B**). The new NC10-pmoA239F-NC10-pmoA590R was only used for Illumina MiSeq-based community analyses but not quantification due to non-target PCR amplicons in several qPCR products.

pmoA sequencing libraries were produced according to the work flow of Han et al. (2020), which included an initial booster PCR to obtain similar amplicon concentrations across all samples, and was followed by tailed-primer PCRs (10 cycles) and index PCRs (8 cycles). For the 25- μ L PCR reaction mixtures the hot start version of the TaKaRa Ex Taq DNA polymerase was used. Reaction mixtures consisted of 2.5 μ L 10x Ex Taq Buffer, 2 μ L dNTP solution (2.5 mM each), 0.75 μ L of each primer mixture (10 μ M concentrations), 2 μ L of bovine serum albumin (1 mg ml⁻¹), 0.125 μ L of TaKaRa Ex Taq HS, 2 μ L of DNA extract, and 14.9 μ L of molecular-grade water (for PCR protocols see **Table 2C**). Paired-end sequencing (600 cycles) was done using a MiSeq Personal Sequencer (Illumina, San Diego, CA).

Amplicon Sequence Data Processing

All DNA sequence data were processed according to the pipeline outlined in Han et al. (2020). Briefly, raw reads were quality-checked by FastQC, followed by read end trimming by seqtk. Trimmed reads were then merged into amplicons by flash (max mismatches density, 0.15) and primer sites removed by usearch (in-silico PCR). Quality filtering was done by prinseq (GC range, 30–70; Min Q mean, 20). OTUs were then clustered according to 97% similarity thresholds (proxy for species-level) to a final number of 927 representative sequences using the USEARCH otutab (), which was also used to remove chimeric sequences. OTU sequences were then used for phylogenetic and bioinformatic analyses.

pmoA Sequences From Lake Metagenomes

To identify potential blind spots or phylogenetic biases of the *pmoA* primer combinations used, we performed complementary *pmoA* analyses on lake sedimentary metagenomes. Metagenomes of DNA extracts from five sediment depths of the deepest station in each lake were sequenced at the Joint Genome Institute (JGI; Berkeley, CA, United States; **Supplementary Table S1**). Paired sequence reads were generated on an Illumina NovaSeq S4 sequencer in 2 \times 150 bp mode. Assembly and annotation were performed by the standard automated pipeline of the JGI (see **Supplementary Material**) and loaded into the Integrated Microbial Genomes and Metagenomes (IMG/M) platform (Chen et al., 2021) for exploration and systematic gene search. Potential *pmoA* genes from all 25 metagenomes were identified by the AMO Pfam motif (PF02461) detected in the encoded proteins by the IMG annotation pipeline (Chen et al.,

2021) resulting in 105 genes in total. The sequences were downloaded and dereplicated (100% nucleotide sequence identity) with Vsearch (v.2.14.1; Rognes et al., 2016) using standard settings, resulting in 81 unique sequences. *pmoA* genes were distinguished from similar *amoA* (ammonia monooxygenase subunit A genes) based on their placement in phylogenetic trees (see below).

pmoA Phylogenetic Analyses

Taxonomic assignments were performed using a newly constructed, comprehensive and up-to-date *pmoA* sequence alignment database in ARB (Ludwig et al., 2004). This database included published *pmoA* amplicon and metagenome sequences and was initially based on an alignment produced on a subset of sequences using ClustalW in SeaView. This gene data base has since been expanded to include >5,000 *pmoA* sequences in addition to representatives of *pmoA*-like RA21 and *pxmA* (putative copper-containing monooxygenase) and *amoA* gene clusters. In the process of database expansion, the overall alignment has been updated and optimized. All amplicon sequences obtained with the general *pmoA* and NC10-specific primer pairs and metagenomic *pmoA* sequences were added and aligned to the curated *pmoA* database. De-novo phylogenetic trees, calculated using ARB Neighbour-Joining with Jukes-Cantor Correction (1,000 bootstraps), were then used to taxonomically classify all *pmoA* OTUs to the genus-level. Tree calculations were based on a ~470-base pair region that corresponds to the amplified region of the A189F-Mb661R primer pair.

Sequence Annotations and Accession Numbers

All *pmoA* OTU taxonomic assignments are shown in **Supplementary Material S1**. Amplicon sequences are publicly accessible at the NCBI Sequence Read Archive (SRA) under Bioproject ID PRJNA785131. Samples used for metagenomes can be found under the ID Gs0142423 on JGI GOLD (<https://gold.jgi.doe.gov/>, Mukherjee et al., 2021). Metagenomic datasets are publicly available at the JGI genome portal (<https://genome.jgi.doe.gov/portal/>) under the proposal Id 504756 and at NCBI (PRJNA620348-PRJNA620356, PRJNA620360-PRJNA620364, PRJNA654670-PRJNA654680).

Data Visualizations and Statistical Analyses

Diversity and richness indices were calculated with the functions “diversity” and “specnumber” in the R-package vegan (v. 2.5–7 (Oksanen et al., 2020)). Kruskal–Wallis tests, combined with Dunn’s posthoc tests with Bonferroni P correction, were performed to check for significant differences in methane concentrations, *pmoA* copy numbers, and *pmoA*/16S rRNA gene ratios in relation to trophic state using R stats version 4.0.3 and the R-package FSA (Ogle et al., 2021). Non-parametric Kruskal–Wallis tests were used instead of One-way Analyses of Variance (ANOVA) due to non-normal data distributions. To test for significant relationships between MOB community composition and sediment depth, used as a

proxy for geochemical gradients, and trophic state at the time of sediment deposition, Permutational Multi-variate Analyses Of Variance (PERMANOVA) were performed on genus- and OTU-level community compositions. PERMANOVAs were performed in R with the `adonis2()` function in `vegan` based on Bray-Curtis dissimilarities (9,999 permutations). An Analysis of Similarity (ANOSIM; Bray-Curtis, 9,999 permutations) was used to test for significant differences in MOB communities between individual trophic state categories (eutrophic, mesotrophic, oligotrophic) using the `anosim()` function in `vegan`. Non-linear Multi-Dimensional Scaling (NMDS) analyses based on Bray-Curtis dissimilarities (Beals, 1984) were performed using the 'metaMDS' function of `vegan` and used to examine community dissimilarities between samples. Similarity percentage (SIMPER) analyses with the 'simper' function (999 permutations) in `vegan` were used to identify genus-level taxa and OTUs that contribute significantly to community dissimilarities between sample categories (i.e., trophic state, respiration zone). To identify potential syntrophic interactions between methanotrophic and methylotrophic microorganisms, correlations between the abundances of dominant MOB taxa and OTUs and potentially methylotrophic bacteria were determined based on Spearman's rank correlation coefficients. The latter were calculated according to Lloréns-Rico et al. (2021) with the `correlation.R` script (https://github.com/raeslab/benchmark_microbiome_transformations/tree/master/scripts/, accessed on 3 July 2021).

All plots were generated with `ggplot2` R-package (<https://ggplot2.tidyverse.org>; Wickham (2016)), basic R plotting functions, LibreOffice Calc, and Microsoft Excel.

Diffusive Fluxes of Methane and O₂

Diffusive porewater fluxes of methane and O₂ across the sediment-water interface were calculated from vertical concentration profiles using a one-dimensional reaction-transport model (Müller et al., 2003; equation 5) applying published diffusion coefficients (D_{O₂} (5°C): 1.25 × 10⁻⁵ cm² s⁻¹ (Müller et al., 2003); D_{CH₄} (5°C): 9.5 × 10⁻⁶ cm² s⁻¹ (Lerman, 1979)). An empirical formation factor F of 1.2 (Maerki et al., 2004) was used to correct for porosity and tortuosity of the sediment.

Thermodynamic Calculations

Standard Gibbs energies of potential aerobic and denitrifying methanotrophic reactions, and widespread, potentially competing aerobic organotrophic and lithotrophic reactions, were calculated based on ΔG_r[°] values published in Thauer et al. (1977). The range of *in situ* Gibbs energies (ΔG_r[']) of these reactions in lake sediments was calculated for a range of environmentally relevant educt and product concentrations according to the equation

$$\Delta G_r' = \Delta G_r^\circ + RT \ln Q_r$$

where R is the universal gas constant (0.008314 kJ mol⁻¹ K⁻¹), T is standard temperature (298.15K), and Q_r is the reaction quotient. For further details, see Table 5.

RESULTS

Methane Concentration Profiles and Potential for Aerobic Methanotrophy

Porewater-dissolved methane concentrations increased with trophic state, with sediment depth, and in several cases with station water depth (Lake Zug, Lake Zurich, Lake Lucerne; Figure 1A). Eutrophic lakes (Lakes Greifen, Baldegg, and Zug) had higher methane concentrations than the oligotrophic Lake Lucerne (*p* < 0.001, Kruskal–Wallis test followed by a Dunn's post hoc test). The highly eutrophic Lake Greifen and Lake Baldegg individually also had higher methane concentrations than Lake Lucerne (*p* < 0.05, same test).

All stations in the eutrophic lakes and the hypoxic deep station in Lake Zurich displayed steep increases in methane concentrations from the sediment surface downward. This and the concave-down shapes of these concentration profiles indicate that net methane production sets in within the top 1 cm of sediment at these stations. These stations also had elevated methane concentrations all the way to the shallowest sampling interval (0–0.5 cm sediment depth). By contrast, methane concentrations at the middle and shallow stations in mesotrophic Lake Zurich and all stations in oligotrophic Lake Lucerne remained at lower levels (<0.5 mM) in the top cm. These stations only showed strong methane concentration increases, combined with downward concavity indicative of net methane production, below 2–4 cm.

Matching the methane concentration profiles, modeled methane fluxes increase with trophic state (Figure 2A; Table 3). The highest methane fluxes were detected at the deepest stations of all lakes except the year-round artificially aerated Lake Baldegg. By contrast dissolved O₂ fluxes into sediments did not change clearly with trophic state (Figure 2B). O₂ fluxes were consistently higher in eutrophic Lake Baldegg and Lake Zug compared to oligotrophic Lake Lucerne. The lowest O₂ fluxes were measured at the seasonally and permanently hypoxic deep stations of Lake Greifen and Lake Zurich, respectively. Ratios of methane to O₂ fluxes reflect the high methane fluxes and low O₂ fluxes at these two deep hypoxic stations (Figure 2C), where six times more (Lake Greifen) or equal amounts of methane (Lake Zurich) diffuse to the sediment surface as can be consumed by aerobic methane oxidation under the standard 1:2 stoichiometry of methane to O₂. This is not the case for the remaining 13 stations, where – assuming 1:2 stoichiometry – at most 6–30% of O₂ consumption can be accounted for by aerobic methane oxidation.

Trends in Absolute and Relative Abundances of MOB

Copy numbers of *pmoA*, which we used as a proxy for MOB abundance, generally ranged from 10⁴ to 10⁶ g⁻¹ wet sediment and had their highest values in the top 10 cm (Figure 1B). Hereby, *pmoA* copy numbers varied between and within stations, but did not show consistent trends in relation to redox conditions or sediment depth. Consequently, *pmoA*

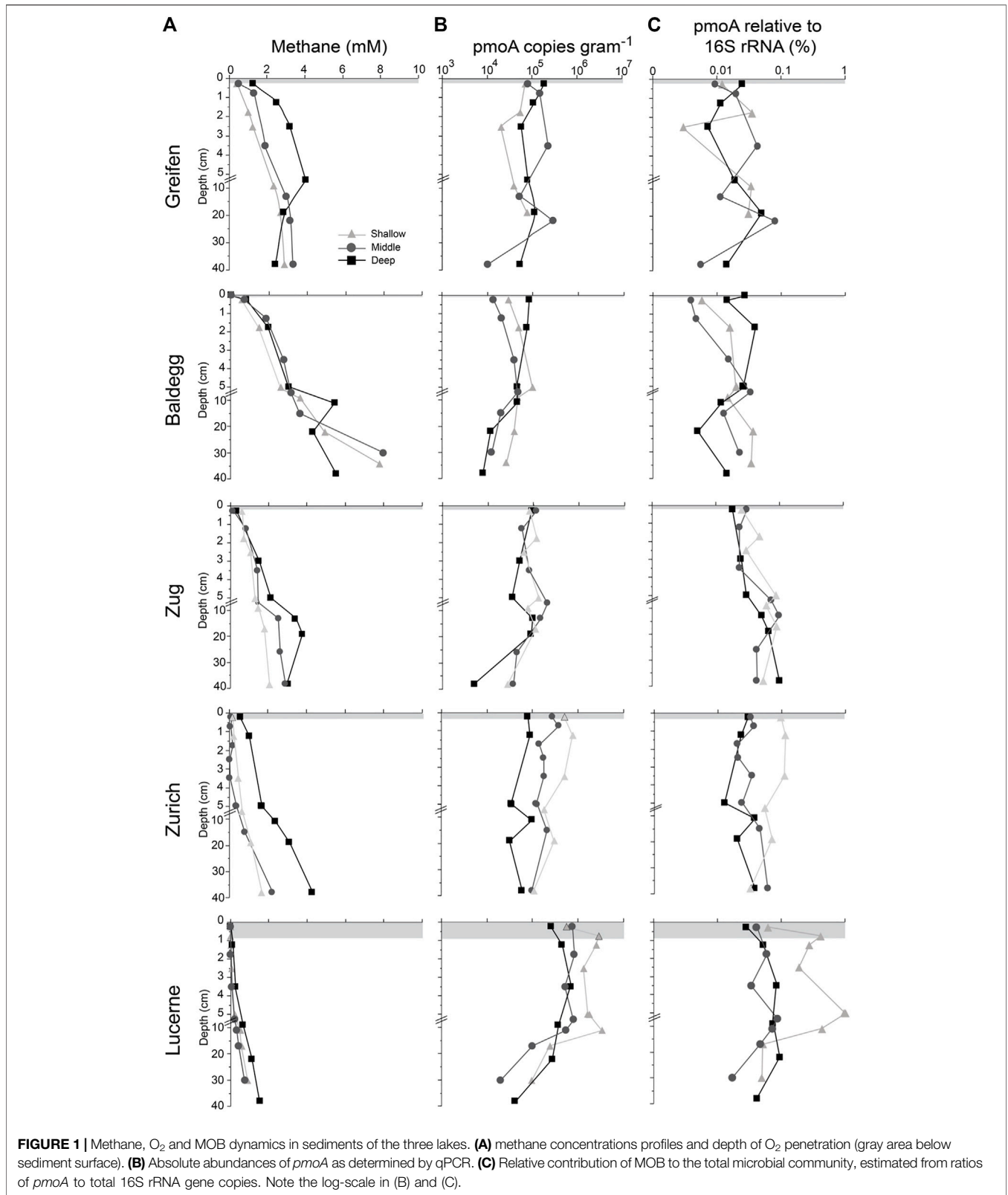
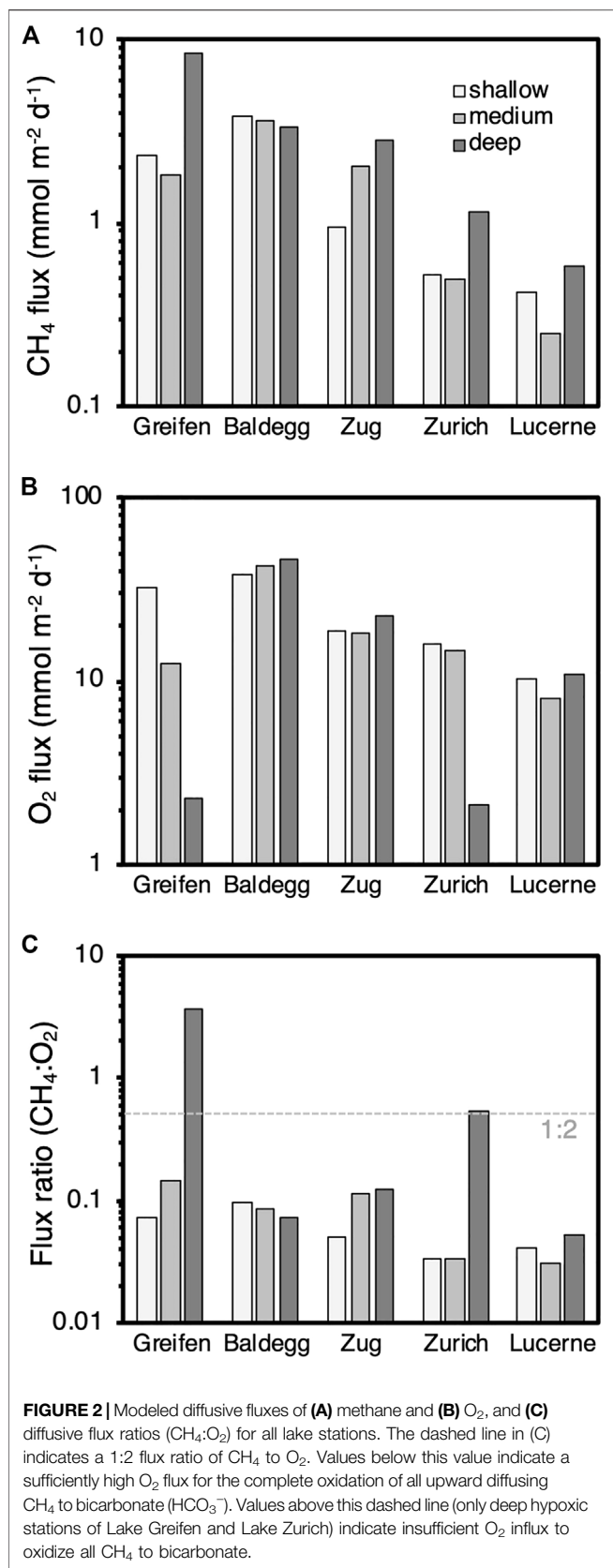


FIGURE 1 | Methane, O₂ and MOB dynamics in sediments of the three lakes. **(A)** methane concentrations profiles and depth of O₂ penetration (gray area below sediment surface). **(B)** Absolute abundances of *pmoA* as determined by qPCR. **(C)** Relative contribution of MOB to the total microbial community, estimated from ratios of *pmoA* to total 16S rRNA gene copies. Note the log-scale in (B) and (C).

copy numbers did not change significantly from oxic sediments to the shallowest samples below the depth of O₂ depletion ($p > 0.05$, here and following paragraphs:

Kruskal-Wallis with Dunn's post hoc test). Furthermore, several sites had bimodal distributions, with surface and subsurface sedimentary *pmoA* copy number peaks, with the



latter generally found in the zone of net methane production (methanogenesis zone).

Despite having the lowest methane fluxes (Figure 2; Table 3), Lake Lucerne had the highest *pmoA* copy numbers (Figure 1B, $p < 0.001$). These were up to 10-fold higher compared to the other lakes, both within and below the O₂ penetration depth. By contrast, in Lake Baldegg, which had the highest methane fluxes (with Lake Greifen) and highest O₂ fluxes (Table 3; Figure 2), and the shallowest O₂ penetration (Table 1), *pmoA* copy numbers were the lowest of all lakes. These trends were statistically supported. The oligotrophic lake (Lake Lucerne) had significantly higher *pmoA* copy numbers than the combined eutrophic lakes ($p < 0.001$), but not Lake Zurich. Both Lake Zurich and Lake Lucerne also had higher *pmoA* copy numbers when individually compared to Lake Baldegg ($p < 0.05$ and $p < 0.001$, respectively).

The contribution of MOB to the total microbial community, expressed in % based on the ratio between *pmoA* and 16S rRNA gene copy numbers, ranged from ~0.005 to 1% and was also highest in Lake Lucerne (Figure 1C). The highest values were reached at the shallow station in Lake Lucerne, despite the low methane concentrations (<2 mM; Figure 1A) and low methane fluxes (Table 3A) at this station. As for *pmoA* copies, Lake Lucerne had significantly higher contributions of MOB compared to the eutrophic lakes ($p < 0.05$), and when compared individually to Lake Baldegg ($p < 0.01$).

Phylogenetic Diversity of Methanotrophic Bacteria Based on *pmoA*

Phylogenetic analyses of *pmoA* sequences obtained by amplicon and metagenome sequencing revealed a phylogenetically diverse MOB assemblage (Figure 3). Groups detected include Type I and Type II MOB, Methylospirales, and less known *pmoA*-like gene clusters (RA21-like, pxma (putative copper-containing monooxygenase)).

Within the gammaproteobacterial Type I methanotrophs, diverse Type Ia and Type Ib OTUs dominated. All of these OTUs cluster more or less closely with Type Ia and Type Ib genera of the family Methylococcaceae, with the exception of several (represented by OTU_130) that cluster in the phylogenetic vicinity of *Candidatus Crenothrix polyspora*. Even though the latter is not phylogenetically separated from typical Type Ia Methylococcaceae *pmoA* (Figure 3) or 16S rRNA gene sequences (Supplementary Figure S3), it is often placed in its own family (Crenotricaceae) due to its distinct morphology. In addition to Type Ia and Type Ib *pmoA* sequences, Type I OTUs belonging to an unknown group (OTU_834) and the USC-gamma cluster were detected. Furthermore, one subcluster that was closely related to *Methylobacter tundripaludicum* was only detected by metagenome sequencing. Closest relatives of the detected Type I MOB OTUs were isolated or sequenced from diverse aquatic freshwater and marine water columns and sediments, as well as wetland and terrestrial soils.

TABLE 3 | Modeled CH₄ and O₂ fluxes and flux ratios by lake and station.

(A)	Shallow			Middle			Deep		
	CH ₄ flux	O ₂ flux	Flux ratio	CH ₄ flux	O ₂ flux	Flux ratio	CH ₄ flux	O ₂ flux	Flux ratio
	mmol m ⁻² d ⁻¹	mmol m ⁻² d ⁻¹	CH ₄ : O ₂	mmol m ⁻² d ⁻¹	mmol m ⁻² d ⁻¹	CH ₄ : O ₂	mmol m ⁻² d ⁻¹	mmol m ⁻² d ⁻¹	CH ₄ : O ₂
Greifen	2.34	32.71	0.07	1.83	12.56	0.15	8.48	2.32	3.65
Baldegg	3.76	38.28	0.10	3.62	42.72	0.08	3.29	46.14	0.07
Zug	0.96	18.64	0.05	2.03	18.01	0.11	2.83	22.57	0.13
Zurich	0.53	15.79	0.03	0.49	14.59	0.03	1.16	2.12	0.55
Lucerne	0.42	10.26	0.04	0.25	8.10	0.03	0.58	10.99	0.05

(B)	Average ± SD		
	CH ₄ flux	O ₂ flux	Flux ratio
	mmol m ⁻² d ⁻¹	mmol m ⁻² d ⁻¹	CH ₄ : O ₂
Greifen	4.21 ± 3.70	15.86 ± 15.46	1.29 ± 2.05
Baldegg	3.56 ± 0.24	42.38 ± 3.94	0.08 ± 0.01
Zug	1.94 ± 0.94	19.74 ± 2.47	0.10 ± 0.04
Zurich	0.73 ± 0.37	10.83 ± 7.57	0.20 ± 0.30
Lucerne	0.41 ± 0.16	9.78 ± 1.50	0.04 ± 0.01

(A) Modeled CH₄ and O₂ fluxes and flux ratios by lake and station. (B) Lake-specific average ± standard deviation (SD) of modeled CH₄ and O₂ fluxes and flux ratios shown in (A). At the standard stoichiometry for aerobic methane oxidation 2 O₂ are reduced per CH₄ oxidized. Thus, at a flux ratio of 0.03, approximately 6% of O₂ that enters sediments is consumed by aerobic methane oxidation, assuming that all methane is oxidized in sediments via the standard stoichiometry of aerobic methane oxidation.

Within the alphaproteobacterial Type II MOB, which had a lower OTU diversity than the gammaproteobacterial Type I MOB, *pmoA* sequences were dominated by the *pmoA1* and *pmoA2* clusters (collectively also known as Type IIa MOB). *pmoA1* and *pmoA2* encode different isoenzymes of pMMO and are found in the genera *Methylocystis* and *Methylosinus*, some members of which have both genes. In addition, we detected sequences that clustered with the genus *Methylocapsa* (also known as Type IIb cluster) and the less known USC-alpha cluster. Despite the known discrimination of the A1809/Mb66a primer pair against USC-alpha and *Methylocapsa*-like *pmoA* (Knief, 2015), metagenome sequencing did not yield any missing OTUs or phylogenetic clusters. The majority of Type II MOB sequences cluster with isolates and environmental sequences from terrestrial and wetland soils.

The new NC10-specific *pmoA29F/590R* primer combination detected sequences that cover the known phylogenetic diversity of NC10-*pmoA*. The fact that NC10 were also detected by metagenome sequencing, including one sequence with 100% sequence identity to *Candidatus Methyloirabilis limnetica*, indicates that this group occurred in significant numbers in certain samples (discussed more later). Detected NC10-*pmoA* sequences clustered with ones that were previously recovered from water-logged soils and aquatic sediments.

Two additional, *pmoA*-like clusters (RA21-like, *pxma*) were only detected by metagenome sequencing, matching past observations that the general A1809/Mb66a misses both of these divergent, functionally poorly understood *pmoA* clusters. The recovered sequences diverge strongly from previously published RA21-like

or *pxma* metagenome sequences and are thus of unknown taxonomic origin.

Lake-specific Trends in *pmoA* OTU Richness, Diversity and Evenness

The methanotrophic community detected with the general A1809/Mb66a *pmoA* primer pair showed a similar OTU richness across the five lakes (Figure 4A; $p > 0.05$, Kruskal-Wallis test followed by a Dunn's post hoc test). The diversity and evenness was, however, significantly lower in oligotrophic Lake Lucerne compared to each of the other lakes (Figures 4B,C; $p < 0.001$, same tests). This indicates that, despite harboring a comparable total number of OTUs, MOB communities in Lake Lucerne are dominated by few highly abundant OTUs. By contrast, the other four lakes shared a similar, higher evenness and diversity of OTUs. Richness and diversity comparisons were not performed on NC10, as only 19 OTUs belonging to this phylum were recovered, most of which were unique to sediments of Lake Lucerne.

Depth Zonation and Trophic Preference of Methanotrophic Communities

pmoA taxonomic compositions based on the general A1809/Mb66a *pmoA* primer pair showed systematic trends in relation to sediment depth and to a lesser degree trophic state (Figure 5). Clear trends within lakes in relation to water depth or from oxic to anoxic sediment layers within the same sediment cores were absent.

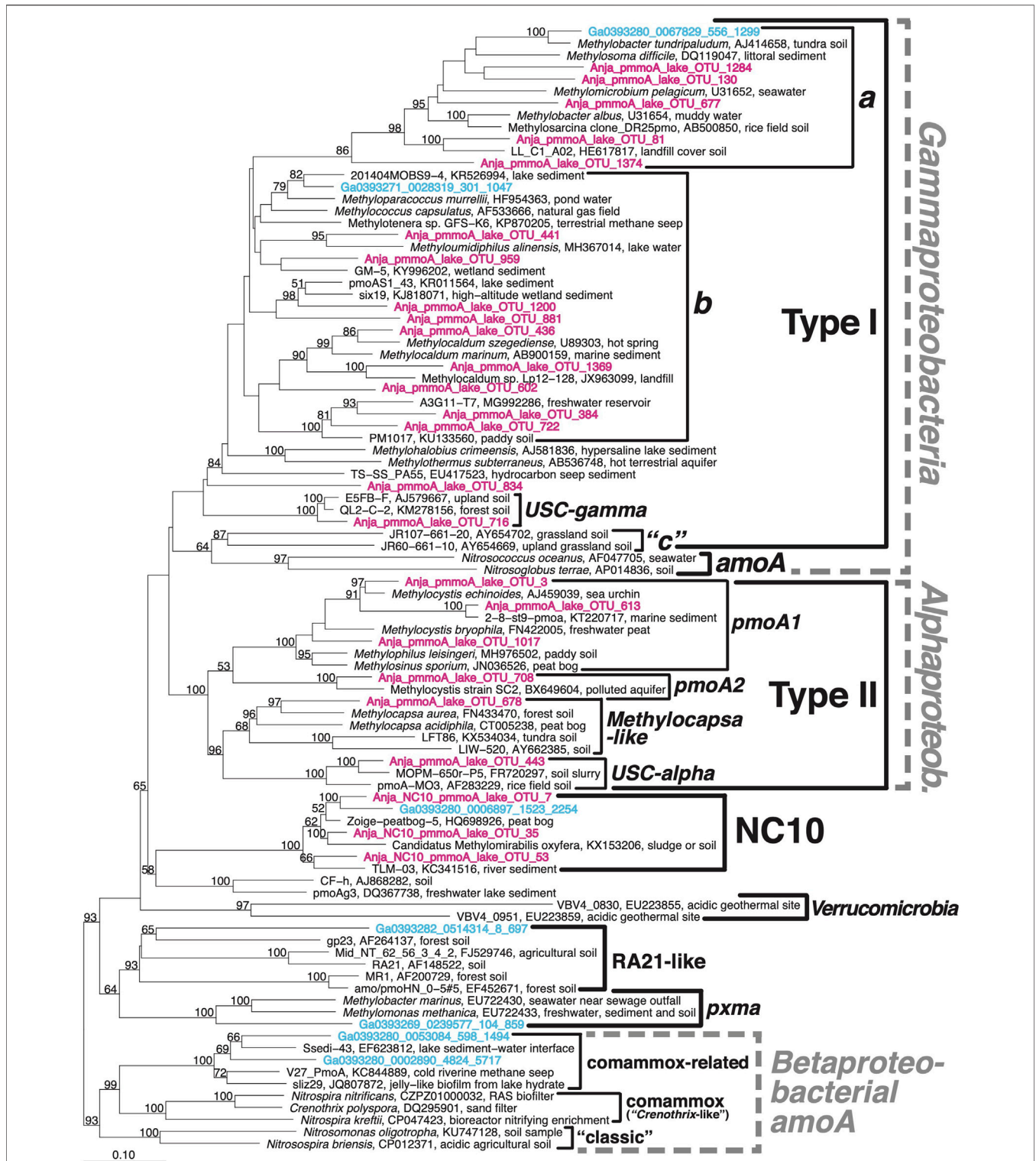
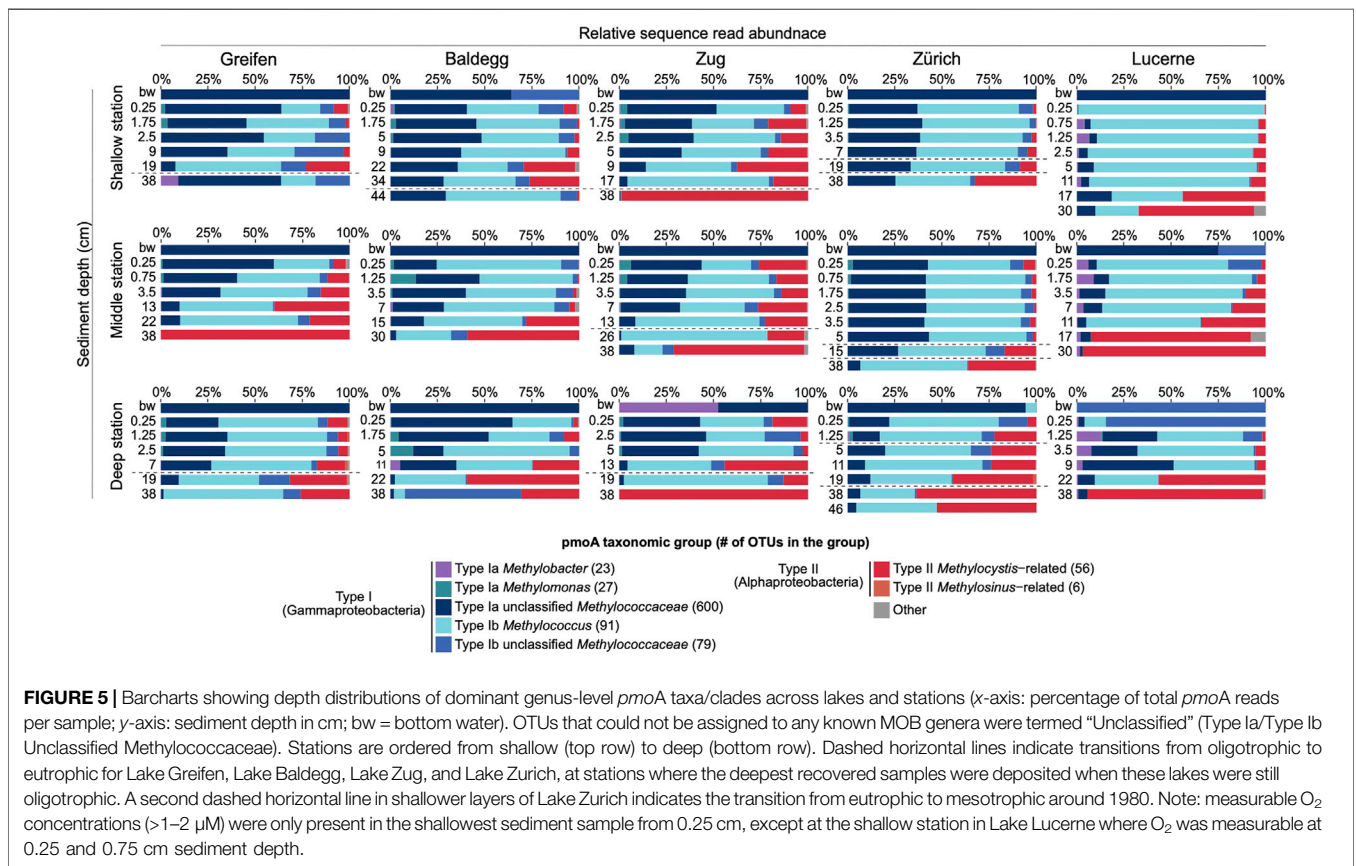
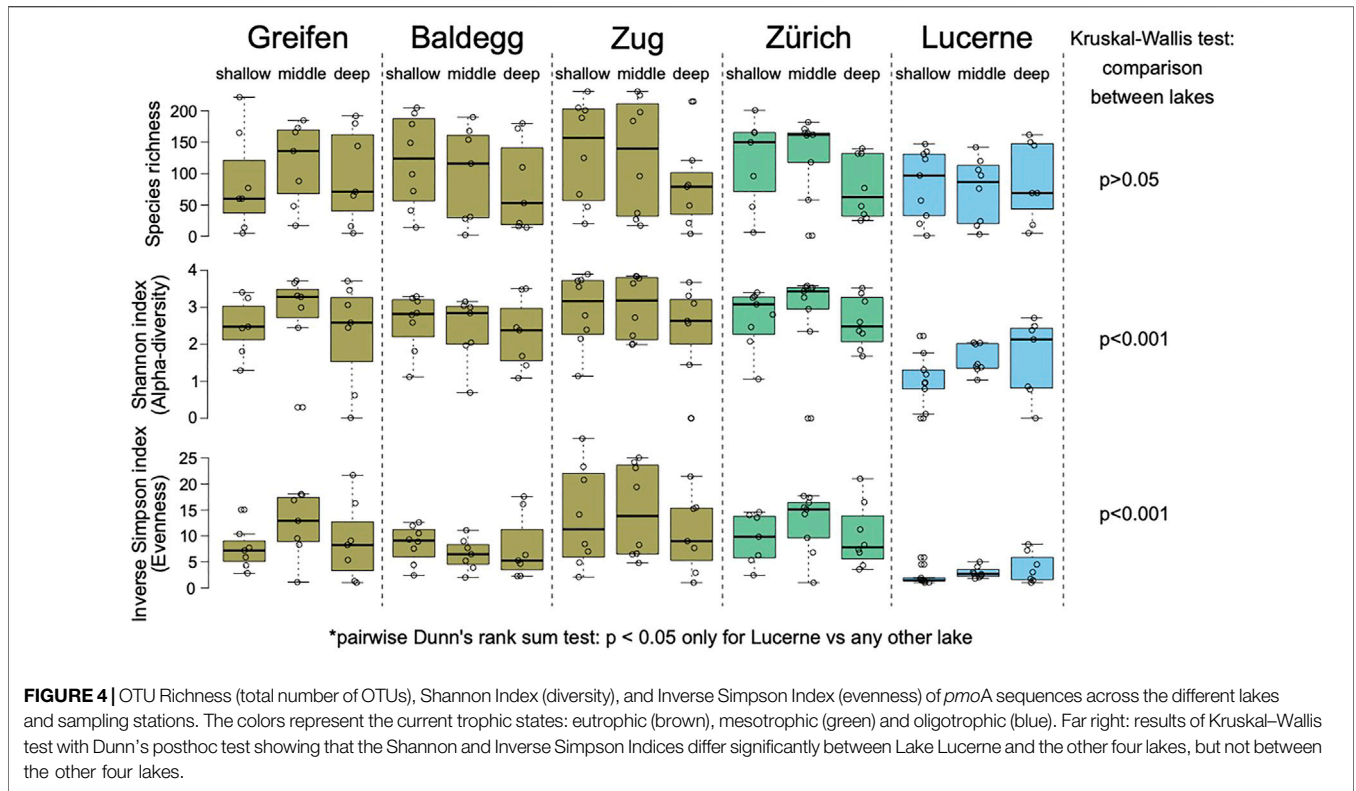


FIGURE 3 | Neighbour-joining phylogenetic tree of *pmoA* amplicon sequences obtained using the general A1809/Mb66a and NC10-specific *pmoA*29F/590R primer combinations (pink) as well as metagenomic *pmoA* sequences (blue). The latter are only shown in cases where metagenomic analyses revealed the presence of *pmoA* (sub)clusters that were not detected by amplicon sequencing. Branching patterns with $\geq 50\%$ bootstrap support (1,000 replicate calculations) are indicated at branch nodes.



Type I methanotrophic communities in all five lakes were generally dominated by three taxonomic groups, termed Type Ia Unclassified Methylococcaceae, Type Ib *Methylococcus*, and Type Ib Unclassified Methylococcaceae (Figure 5). Bottom water was dominated by Type Ia Unclassified Methylococcaceae (in most cases >95% of reads). Exceptions are the deep stations in Lake Zug and Lake Lucerne, which are dominated by Type Ia *Methylobacter* and Type Ib Unclassified Methylococcaceae *pmoA* sequences, respectively. Communities shift systematically from bottom water into sediments, where *pmoA* sequences that cluster with the genus *Methylococcus* (Type Ib), which were nearly absent from bottom water, emerge as a second dominant group.

Percentages of Type Ia Unclassified Methylococcaceae are on average higher in sediments of today's eu- and mesotrophic lakes compared to oligotrophic Lake Lucerne. Percentages of this group also decrease gradually with sediment depth at most stations, although these decreases do not closely match depth distributions of O₂ or anaerobic respiration reactions, or past shifts in trophic state. Similar depth- or trophic state-related changes in Type Ib *Methylococcus*-type *pmoA* contributions are less evident, though, notably, this cluster drops in relative abundances in deep sediment layers of oligotrophic Lake Lucerne and most deep oligotrophic layers of today's eutrophic lakes. The third major Type I cluster (Type Ib Unclassified Methylococcaceae) fluctuates in percentages without clear trends in relation to O₂ or respiration zone, sediment depth, past or present trophic state. Other Type I clusters that accounted for significant, but minor percentages of *pmoA* reads included Type Ia *Methylomonas*- and *Methylobacter*-like sequences, Type Ib *Methylocaldum*-like sequences, and Unclassified Type I-sequences (Figure 5). Read percentages of these groups also did not show clear trends in relation to O₂ or respiration zone, sediment depth, past or present trophic state.

The general decreases in Type I *pmoA* sequence percentages with sediment depth coincided with strong increases in facultative Type II methanotrophs that mainly grouped with the *Methylocystis*-type *pmoA1* cluster (Figure 5). This cluster was almost absent from bottom water but – independent of trophic state – became dominant below the depths of O₂, nitrate, and sulfate depletion in iron-reducing and methanogenic sediment layers.

Comparative Analyses of MOB Based on 16S rRNA Gene Sequences

We checked whether sedimentary trends in *pmoA* sequences were reproducible in the complementary 16S rRNA gene data of Han et al. (2020), and how MOB that were missed by the general A1809/Mb66a *pmoA* primer pair compared in relative abundances (Supplementary Figure S1). These analyses confirm the shift in dominance from gammaproteobacterial to alphaproteobacterial MOB with increasing sediment depth (and age) observed in *pmoA* sequence compositions. Moreover, in sediments of Lake Lucerne, members of Candidatus *Methylomirabilia* (NC10) dominate shallow sediments along with Type Ia Methylococcaceae. *Methylomirabilia* furthermore account for up to ~30% of methanotrophic 16S reads in deep

sediment layers of the eutrophic lakes, and even dominate sediments below 5 cm depth in Lake Zurich. All *Methylomirabilia*-related 16S rRNA gene sequences could be assigned to the order *Methylomirabiales*. Most reads in Lake Lucerne belong to the genus *Methylomirabilis*, while most reads in the other lakes group with the uncharacterized Sh765B-TzT-35 cluster.

A striking difference to the *pmoA* analyses was the much lower percentage of Type Ib in the 16S rRNA gene data set. In addition, alphaproteobacterial Type II were dominated by 16S rRNA sequences that cluster with the mostly methylotrophic genus *Methyloceanibacter* (family: *Methyloligellaceae*), which only includes one confirmed methanotrophic member that, however, lacks *pmoA* (*M.oceanibacter methanicus*; Vekeman et al., 2016). By comparison, percentages of sequences related to facultatively methanotrophic *Methylocystis* are much lower, though these also increase with sediment depth. Lastly, 16S rRNA gene data indicate the presence of low read fractions (~0.1%) of Type III methanotrophs (*Methylacidiphilaceae*; *Verrucomicrobia*) in surface layers of the middle stations in Lake Baldegg and Lake Lucerne.

Taxonomic and OTU-Level Environmental Clustering of *pmoA* Sequences

A Non-linear Multi-dimensional scaling (NMDS) ordination of samples based on major taxa recovered with the general A1809/Mb66a *pmoA* primer pair confirms the main inference from Figure 5 that MOB communities at the genus-level are more strongly structured in relation to sediment depth than trophic state (Figure 6A). This is confirmed based on the results of a PERMANOVA (Table 4). These show that while both sediment depth and trophic state have a significant impact on MOB community structure at the genus-level (both $p < 0.001$), depth explains a higher portion of the observed community variation ($R^2 = 0.22$) than trophic state ($R^2 = 0.16$). Complementary ANOSIM analyses, moreover, show that trophic state at the time of deposition only shows significant differences between samples that were deposited under oligotrophic vs. eutrophic conditions ($R = 0.30$, $p < 0.001$), but not between eutrophic and mesotrophic ($R = 0.08$, $p > 0.05$) or mesotrophic and oligotrophic conditions ($R = -0.16$, $p > 0.05$).

The pattern shifts when NMDS analyses are performed at the OTU-level ("species-level"; Figure 6B). Here trophic state is more strongly correlated with community structure than sediment depth, as indicated by the clear separation of oligotrophic Lake Lucerne from the other four lakes. By contrast, OTU compositions of sediment samples that were deposited under mesotrophic conditions in Lake Zurich are highly similar to samples deposited under eutrophic conditions in Lake Zurich or the other presently eutrophic lakes. Interestingly, OTU samples from the deep oligotrophic layers in Lake Zug and one deep oligotrophic layer in Lake Greifen cluster most closely with oligotrophic communities from Lake Lucerne (Figure 6B), suggesting that trophic state at the time of deposition is the key driver of MOB community structure at

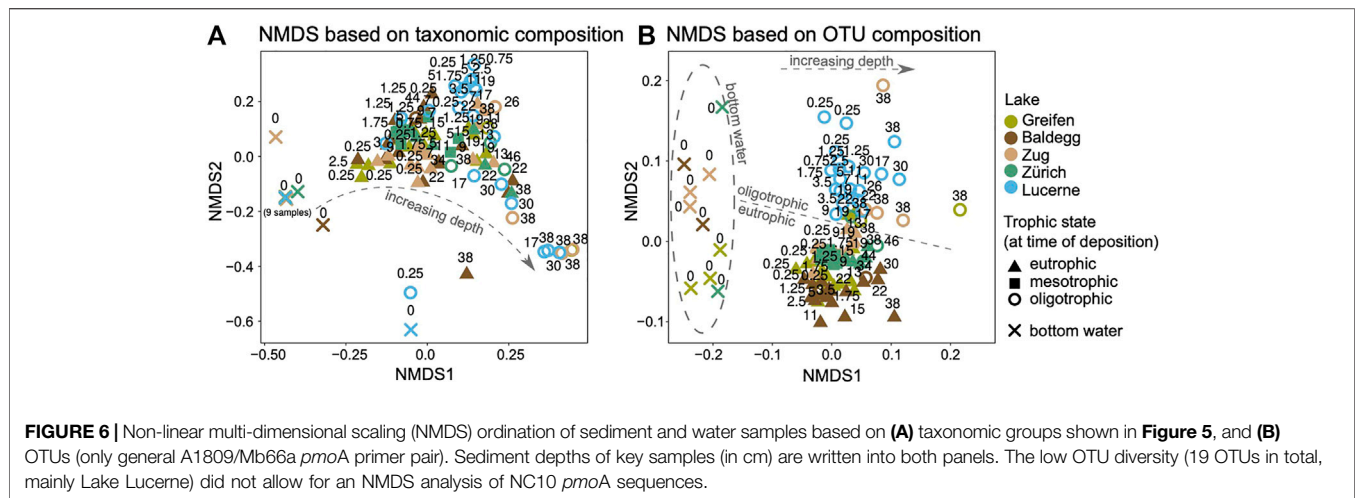


TABLE 4 | Permutational Multi-variate Analysis of Variance (PERMANOVA) results for differences in community composition in relation to trophic state at time of deposition and sediment depth (as a proxy for vertical respiration zone gradients). Taxa-level tests were used as a proxy for MOB community trends at the genus-level, while OTU-level tests were used as a proxy for community trends at the species-level. [*** indicates $p < 0.001$].

		Degrees of freedom	Sums of squares	Mean squares	F-model	R^2	p
Taxa	Trophic state	2	1.71	0.85	12.34	0.16	***
	Sediment depth	1	2.2	2.2	31.78	0.21	***
	Residuals	95	6.56	0.07	0.63		
	Total	98	10.46	1			
OTUs	Trophic state	2	7.34	3.67	15.54	0.23	***
	Sediment depth	1	2.68	2.68	11.36	0.08	***
	Residuals	95	22.42	0.24	0.69		
	Total	98	32.44	1			

the OTU-level. This is confirmed based on a PERMANOVA test (Table 4), which shows that while both sediment depth and trophic state have a significant impact on MOB community structure at the OTU-level (both $p < 0.001$), trophic state explains a much higher portion of the observed community variation ($R^2 = 0.23$) than sediment depth ($R^2 = 0.08$).

Further OTU-level analyses, reveal that the three main *pmoA* clusters (Figure 5; Type Ia unclassified Methylococcaceae, Type Ib *Methylococcus*, Type II *Methylocystis*) in eu- and mesotrophic lakes are dominated by a larger number of OTUs than in Lake Lucerne (Supplementary Figure S2). Most of these dominant OTUs in the eu- and mesotrophic lakes are shared among these lakes. By contrast, as already indicated by Figure 4, Lake Lucerne is dominated by a smaller number of OTUs with very high relative abundances. These dominant OTUs in Lake Lucerne represent a subset of the OTUs that dominate sediments of the eu- and mesotrophic lakes. Additional similarity percentage (SIMPER) analyses reveal that some OTUs are highly abundant in oligotrophic samples of Lake Lucerne and deep oligotrophic layers of Lakes Greifen, Baldegg, and Zug, but nearly absent from sediment layers that were deposited under

eutrophic conditions (e.g. Methylococcaceae OTU2, *Methylocystis*-related OTU3; Supplementary Figure S2).

Potential Environmental and Biological Drivers of MOB Communities

Abundance analyses of *pmoA* copy numbers and *pmoA*/16S ratios in relation to respiration reactions and trophic state confirm both the absence of a clear *pmoA* copy number relationship with respiration zone as well as the clear relationship between *pmoA* copy number and trophic state (Figure 7A). On average, *pmoA* copy numbers increase by a factor of 8 and *pmoA*/16S ratios increase by a factor of 4 from sediment samples that were deposited under eutrophic conditions to ones that were deposited under oligotrophic conditions. Both increases are significant ($p < 0.001$, Kruskal–Wallis followed by Dunn’s post hoc test).

In addition, dominant *pmoA* taxonomic groups (Figure 5) and their most abundant OTUs show clear patterns in relation to vertical respiration zone and to a lesser degree trophic state (Figure 7A). The observed patterns in relation to respiration

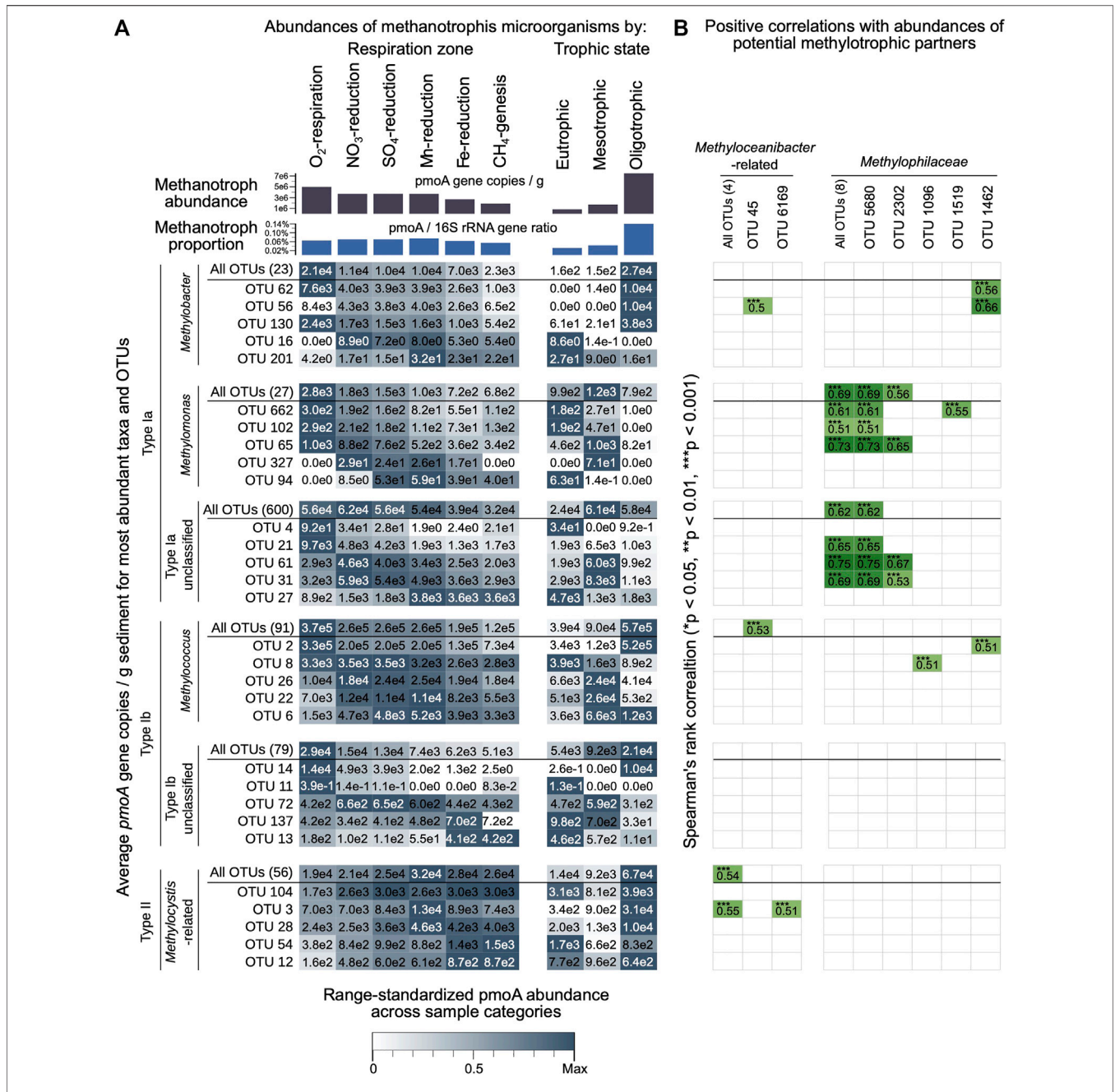


FIGURE 7 | (A) Total *pmoA* copy numbers, relative abundances of *pmoA* relative to 16S rRNA gene copy numbers (bar charts at top), and calculated gene copy numbers of dominant *pmoA* taxa and their five most abundant OTUs across different respiration zones and in relation to lake trophic state at the time of sediment deposition (remaining graph). Total *pmoA* copy numbers and *pmoA*/16S rRNA gene percentages are averages of values shown in **Figures 1B,C**, respectively. Gene copy numbers of dominant *pmoA* taxa and OTUs were calculated by multiplying relative *pmoA* abundances by total *pmoA* copy numbers per gram of wet sediment. The heatmap color intensity reflects the standardized average *pmoA* copy numbers per taxon or OTU, with highest intensity representing the highest average copy number within each comparison (respiration zone, trophic state). **(B)** Spearman correlation matrix of calculated *pmoA* copy numbers per taxon or dominant OTU (calculated as in (A)) vs. calculated 16S rRNA gene copy numbers of dominant methylotrophic taxa (Methylophilaceae, Methyloceanibacter-related) and their dominant OTUs as determined by multiplying 16S rRNA gene sequence contributions by qPCR-based total 16S rRNA gene copy numbers (all 16S data from Han et al., 2020). Spearman's rank correlation coefficients of ≥0.5 are shaded in green and listed in the graph. Asterisks indicate significance level (*p < 0.05; **p < 0.01; ***p < 0.001).

zone explain the observed significant correlations of *pmoA* community structure at the genus- and OTU-level with sediment depth, which *per se* is not a likely community driver (see previous section). The Type Ia MOB genera *Methylobacter*

and *Methylomonas* and Type Ib genus *Methylococcus*, and dominant OTUs within all three genera, have their highest calculated average *pmoA* abundances in oxic sediments. By contrast, the Type Ia Unclassified Methylococcaceae and Type

II *Methylocystis*, and several dominant OTUs within these groups, have peak *pmoA* abundances in denitrifying, sulfate- and manganese-reducing (Unclassified Type Ia) and in manganese- and iron-reducing and methanogenic layers (*Methylocystis*) (Figure 7A). With respect to abundances in relation to trophic state, we generally observe that Type Ia *Methylobacter* and Type II *pmoA* sequences, and their dominant OTUs, reach their peak abundances under oligotrophic conditions, whereas Type Ia *Methylomonas* and Unclassified *Methylococcaceae*, and their dominant OTUs, reach their highest abundances under meso- and eutrophic conditions. Highly similar patterns to those in Figure 7A were observed when calculated absolute abundances of dominant taxa and OTUs were substituted with relative abundances (Supplementary Figure S4).

Calculated *pmoA* abundances of major MOB taxa and their dominant OTUs correlate strongly with major methylophilic taxa and their dominant OTUs (Figure 7B). Type Ia Unclassified *Methylococcaceae*, Type Ia *Methylomonas*, and Type Ib *Methylococcus*, as well as dominant OTUs within these three groups, show strong positive Spearman's correlations ($Rho > 0.5$, $p < 0.001$) with 16S rRNA gene-based abundances of *Methylophilaceae* and dominant OTUs of *Methylophilaceae*. In addition, matching their observed *pmoA* peak abundances in deeper layers, *pmoA* abundances of *Methylocystis* and one of its dominant OTUs (OTU_3) are correlated with 16S gene-based abundances of *Methyloceanibacter* and one of its dominant OTUs (OTU_45). Nonetheless, *pmoA* OTUs with highest abundances in the oxic or denitrifying sediment layers (Type Ia and Type Ib MOB) were much more likely to correlate with methylophilic OTUs than *pmoA* OTUs reaching peak abundances in deeper anoxic layers (Type II). Among *pmoA* OTUs with peak abundances in the oxic or denitrifying layer, 19 and 22%, respectively, showed a significant positive correlation ($Rho > 0.5$, $p < 0.05$) with methylophilic 16S OTUs. This proportion dropped to 10 and 9% for OTUs most abundant in the sulfate and manganese reduction zones, and was 0 and 2%, respectively, in the iron reduction and methanogenesis zones. Moreover, of the 64 *Methylocystis* OTUs, it was only the aforementioned OTU_3 (Figure 7B) that showed significant correlations with *Methyloceanibacter*.

We found no clear relationship between trophic state and the percentage of *pmoA* OTUs that correlate significantly with the percentage of methylophilic 16S OTUs ($Rho > 0.5$, $p < 0.05$). Based on calculated absolute abundances, 10 and 12% of *pmoA* OTUs with peak abundances in sediments deposited under eutrophic and oligotrophic conditions, respectively, were significantly correlated with methylophilic.

DISCUSSION

Methanotrophic bacteria play a key role in mediating methane emissions from lakes across the world (Bastviken et al., 2008; Thottathil et al., 2018). Although eutrophication enhances organic carbon inputs to lake sediments (Heathcote and Downing, 2012; Anderson et al., 2014) and increases lake sedimentary methane production and emissions (Beaulieu

et al., 2019; Fiskal et al., 2019), its effects on the activity, abundance, and community structure of sedimentary MOB is not understood. By performing detailed quantitative and phylogenetic analyses on MOB communities in sediment cores from five lakes that span the past centuries, and by analyzing this community data in the context of trophic history, present-day respiration zone distributions, O₂ and methane fluxes, we produce novel insights into the potential controls on MOB communities in lake sediments. We summarize major findings in the following paragraphs and discuss these in further detail in the subsequent thematically structured subsections.

Summary of Major Findings

Matching measured methane concentrations (Figure 1A) and modeled methane production profiles (Fiskal et al., 2019), we observe clear increases in surface sedimentary methane fluxes in eutrophic lakes (Figure 2A; Table 3). Yet, gene copy number-based estimates indicate that MOB are on average 8-fold more abundant and account for 4-fold higher fractions of the total microbial community in samples deposited under oligotrophic compared to eutrophic conditions (Figure 7). An insufficient supply of O₂ can be ruled out as a first-order explanation as, except at the hypoxic deep stations in Lake Greifen and Lake Zurich, only a minor fraction (6–30%) of the diffusive flux of O₂ can be accounted for by aerobic methane oxidation assuming the standard 2:1 stoichiometry of O₂:CH₄ (Figure 2C).

Matching previous studies on lake sediments (Rahalkar et al., 2009; Pester et al., 2011; Tsutsumi et al., 2011; He et al., 2021; Lyautey et al., 2021), *pmoA* copy numbers do not change significantly from oxic to anoxic sediments (Figure 1B). Based on calculated *pmoA* gene copy numbers of individual MOB genera, certain Type II MOB taxa (mainly *Methylocystis*) even reach peak abundances in deep methanogenic and metal reducing sediment (Figure 5; Supplementary Figure S1). The observation of high or even elevated *pmoA* copies below the oxic-anoxic transition is at odds with cultivation data, which indicate that the vast majority of alpha and gammaproteobacterial MOB, including all *Methylocystaceae*, are obligate aerobes (Bowman, 2014). This raises questions concerning whether these *pmoA* sequences belong to catabolically active, dormant, inactive, or even dead cells.

While Type II MOB dominate deeper layers, Type I MOB (*Methylococcaceae*) are the major group in oxic and suboxic bottom water and surface sediments (Figure 6), matching other studies on freshwater surface sediments (e.g., Rahalkar et al., 2009; Lyautey et al., 2021). Hereby the (near) absence of Type Ib, but not Type Ia, MOB in overlying water suggests a habitat preference of Type Ib for sediments. Similar to previous studies (Yang et al., 2016; He et al., 2021; Lyautey et al., 2021), *Methylococcus*-type *pmoA* dominate Type Ib communities. By contrast, *Methylobacter*-type Type Ia sequences, which frequently dominate lake sediments elsewhere (Tsutsumi et al., 2011; Reim et al., 2012; Yang et al., 2016), are less abundant. Instead, the majority of Type Ia sequences fall outside of known genera ('Type Ia Unclassified *Methylococcaceae*'). Some of these sequences cluster loosely with *Candidatus Crenothrix polyspora*

(Figure 3), raising questions regarding their identity as filamentous Crenotrichaceae or unicellular (mostly coccoid) Methylococcaceae. Phylogenetic trees based on both *pmoA* and 16S rRNA gene sequences, in which Crenotrichaceae (Crenothrix polyspora) group with well-known Methylococcaceae isolates (Figure 3, Supplementary Figure S3) could not resolve this issue. Besides Type I and Type II MOB taxa, we detect NC10-type denitrifying methanotrophs (Methylomirabilota) based on 16S rRNA gene analyses (Supplementary Figure S1). Members of the type genus *Methanomirabilis* occur at similar relative abundances to Type I methanotrophs in denitrifying sediments of Lake Lucerne, whereas uncultivated groups of Methylomirabilota (mainly Sh765B–TzT–35) occur at significant abundances in deeper, nitrate-depleted, fully anoxic layers of most lakes.

While the drivers of (uncultivated) Methylomirabilota communities remain uncertain, Type I and Type II MOB taxa at the genus-level show vertical distributions that match distributions of major respiration reactions (Figure 7A and Supplementary Figure S4). This raises the possibility that distributions of MOB genera in lake sediments reflect genus-level differences in the ability to live without O₂ and respire different anaerobic electron acceptors. Moreover, OTU-level analyses indicate lake trophic state as a major driver of MOB diversity and community structure at the species-level (Figure 4, 6B & 7A). Potential explanations are that differences in anabolic nutrient regimes or micro-scale habitat heterogeneity impact MOB communities at the species-level. By contrast, based on correlation analyses of MOB taxa and potential methylotrophic partner organisms (Results text), we find no evidence that co-dependencies of MOB on syntrophic partners vary with trophic state. Instead, correlations between MOB and methylotrophic bacterial OTUs follow clear taxonomic and environmental trends, being most frequently observed within Type I taxa that dominate oxic and suboxic surface sediments.

Explanations for the Higher MOB Gene Copy Numbers and Percentages Under Low CH₄ fluxes

The order of magnitude higher *pmoA* copy numbers in oligotrophic Lake Lucerne compared to the eutrophic lakes (Figure 1B & 7A), show parallels with quantitative data on total microbial community size. Total 16S rRNA gene copy numbers were also highest in Lake Lucerne (Han et al., 2020) and were generally supported by microscopic cell counts which indicated higher microbial cell abundances in Lake Lucerne and Lake Zurich than in the three eutrophic lakes (Fiskal et al., 2019). These trends seem paradoxical given that the higher deposition and burial rates of organic carbon in the eutrophic lakes sustain higher total respiration and methanogenesis rates throughout cores from these lakes (Fiskal et al., 2019). A possible explanation is that microbial cell-specific energy requirements are higher in eutrophic lake sediment, e.g. due to enhanced physiological stress from elevated toxic contaminant loads. Yet, though more research is needed, previous studies suggest minor effects of anthropogenic toxin contamination on sediment microbial

communities (Chen et al., 2014; Di Cesare et al., 2020). Notably also, the shallow and medium station in Lake Zurich are located in a Zinn (Sn)-polluted area (Lennartz, 2010), and yet had high cell counts and high qPCR values of *pmoA* and total 16S genes.

An alternative explanation is that – matching the higher microbial activity – sediments of eutrophic lakes have higher microbial growth rates, but that these coincide with higher rates of mortality, e.g. due to viral lysis or predation. Though we lack data on viral lysis rates, previous work has shown high abundances of oligochaetes (Tubificidae) to 20 cm sediment depth in the three eutrophic lakes and absence of these worms from all but the sediment surface in Lake Lucerne (Fiskal et al., 2021a). Gut microbiome analyses suggest protein-rich diets that are consistent with microbial grazing as a major food source of tubificids (Fiskal et al., 2021a; de Valk et al., 2017). While lake sedimentary invertebrates are known to stimulate growth of MOB in surface sediments (“microbial gardening”), leading to MOB becoming a major food source of these invertebrates in some lakes (Kiyashko et al., 2001; Deines et al., 2007; Jones and Grey, 2011), none of the stations in this study show evidence for MOB gardening (Fiskal et al., 2021a). We thus propose that non-selective grazing by tubificids causes higher mortality and ultimately results in lower abundances of microorganisms, including MOB, in sediments of the eutrophic lakes.

While non-selective grazing by oligochaetes explains lower absolute abundances of MOB, it does not explain the lower relative abundances (percentages) of MOB in the eutrophic lakes (Figure 1C, 7A, and Supplementary Figure S2). These lower percentages are particularly striking given the steep, overlapping O₂ and CH₄ concentration gradients in the top 0.5 cm of eutrophic lakes (Figure 1A), which imply high potential for aerobic methanotrophy. In the following paragraphs, we evaluate three potential hypotheses to explain the lower percentages of MOB in eutrophic lake sediments with high methane fluxes.

Direct observations on sediment cores from the eutrophic lakes revealed the presence of gas bubbles starting just below the 1 to 2 cm thick, flocculent surface layer. While gas bubbles also appeared in sediment of Lake Lucerne and the shallow and medium stations in Lake Zurich, these bubbles were restricted to deeper, more compacted sediment layers and less numerous in these locations. Based on these observations, it is possible that most methane in sediments of eutrophic lakes is present in gas bubbles rather than bioavailable dissolved form. These methane bubbles may bypass the “biological methane filter” in oxic surface sediments by rapid transit through the flocculent surface layer followed by ebullition into overlying water, explaining why methane oxidation only supports a small percentage of the microbial community in eutrophic lake sediments. The importance of ebullitive release of methane from lake sediments to overlying water and the atmosphere is well-known and especially high for shallow and/or eutrophic lakes (Thebrath et al., 1993; Schubert et al., 2012), though little is known about how ebullitive losses quantitatively compare to biological consumption by MOB in lake sediments.

TABLE 5 | Gibbs energies of potential aerobic and denitrifying methanotrophic reactions, organotrophic reactions, and lithotrophic reactions. We include Gibbs energies under standard conditions (ΔG_r°), and for a range of environmentally relevant educt and product concentrations ($\Delta G_r'$ (range), see footnote below table) assuming standard temperature, pressure, and pH (Note: the impact of *in situ* temperature, pressure, and pH on Gibbs energy yields is negligible within the range of calculated educt and product concentrations).

Reaction	kJ mol ⁻¹	
	ΔG_r°	$\Delta G_r'$ (range)
Methanotrophic		
CH ₄ + 2 O ₂ → HCO ₃ ⁻ + H ⁺ + H ₂ O	-813	-811 to -732
CH ₄ + O ₂ → 0.5 CH ₃ COO ⁻ + 0.5 H ⁺ + H ₂ O	-391	-394 to -343
CH ₄ + O ₂ → COO ⁻ + 1.5 H ₂ + H ⁺	-340	-449 to -397
CH ₄ + 0.5 O ₂ → CH ₃ OH	-125	-136 to 99
CH ₄ + 2.67 NO ₂ ⁻ + 1.67 H ⁺ → HCO ₃ ⁻ + 1.33 N ₂ + 2.33 H ₂ O	-923	-829 to -730
Organotrophic		
glucose + 6 O ₂ → 6 HCO ₃ ⁻ + 6 H ⁺	-2,843	-3,015 to -281
aspartic acid + 3 O ₂ + 2 H ₂ O → 4 HCO ₃ ⁻ + NH ₄ ⁺ + 3 H ⁺	-1,351	-1,475 to -1,361
guanine + 2 O ₂ + 10 H ₂ O → 5 HCO ₃ ⁻ + 5 NH ₄ ⁺	-1,006	-1,186 to -1,100
lactate + 3 O ₂ → 3 HCO ₃ ⁻ + 2 H ⁺	-1,322	-1,357 to -1,243
acetate + 2 O ₂ → 2 HCO ₃ ⁻ + H ⁺	-844	-846 to -761
Lithotrophic		
NH ₄ ⁺ + 1.5 O ₂ → NO ₂ ⁻ + 2 H ⁺ + H ₂ O	-274	-343 to -278
NO ₂ ⁻ + 0.5 O ₂ → NO ₃ ⁻	-74	-74 to -31
H ₂ + 0.5 O ₂ → H ₂ O	-237	-203 to -160

There are four small, separate blocks of information under the subheadings "Methanotrophic", "Organotrophic", "Lithotrophic", and "Concentrations of reaction products (product concentrations)". These should be visually separated, e.g. by increasing the line spacing above each of these subheadings. If this table must be shown in two-column width format, then I suggest showing the footnotes in the following, more concise format:

Methanotrophic:

Max: {CH₄} = 10 mM; {O₂} = {NO₂⁻} = 100 μM

Min: {CH₄} = 1 μM; {O₂} = {NO₂⁻} = 1 nM

Organotrophic

Max: {organic compound} = {O₂} = 100 μM

Min: {organic compound} = {O₂} = 1 nM

Lithotrophic:

Max: {NH₄⁺} = 10 mM; {O₂} = {NO₂⁻} = {H₂} = 100 μM

Min: {NH₄⁺} = 1 μM; {O₂} = {NO₂⁻} = {H₂} = 1 nM

Concentrations of reaction products (product concentrations)

{CH₃OH} = {formate} = {acetate} = {NO₃⁻} = 1 μM

{H₂} = 10 nM

{HCO₃⁻} = 2 mM

{N₂} = 100 μM

Given the high sedimentation rates of labile microalgal biomass (Han et al., 2020) and shallow depletion of O₂ and nitrate in the three eutrophic lakes (Table 1), competition for O₂ or nitrate between MOB and other microorganisms could also explain the lower MOB percentages in eutrophic lakes. Thermodynamic calculations (Table 5) indicate that aerobic organotrophic microorganisms have substantially higher energy yields than aerobic or denitrifying MOB. Organotrophs could thus outcompete MOB for O₂ and nitrate, and thereby suppress methane consumption rates and the efficiency of the biological methane filter in the eutrophic lakes. By comparison, sediments of Lake Lucerne have deeper O₂ and nitrate penetration (Table 1) and receive less labile algal organic matter than the eutrophic lakes (Han et al., 2020). Here competition for O₂ or nitrate could be less intense due to stronger electron donor limitation of organotrophs, and lead to MOB being major O₂ consumers. In Lake Lucerne, MOB may even have energetic advantages over competing lithotrophic

nitrifying bacteria (Table 5), which are major microbial community members in this lake (Han et al., 2020). Reduced competition for O₂ and nitrate could also explain why MOB effectively deplete upward-diffusing methane in the surface centimeters of Lake Lucerne and the oxic shallow and medium stations of Lake Zurich.

The third hypothesis concerns potential changes in dominant methanotrophic reactions in relation to trophic state. Besides performing the complete oxidation of methane to CO₂, MOB are known to under certain conditions only partially oxidize methane to low molecular weight intermediates, such as methanol, H₂, formate, or acetate, which are then utilized by denitrifying partner organisms (Kalyuzhnaya et al., 2013; Beck et al., 2013; Oshkin et al., 2014; Hernandez et al., 2015). The factors that determine whether MOB perform complete or partial oxidation are not understood. O₂ concentrations may affect the MOB genera involved, but not necessarily the occurrence

of syntrophic reactions (Beck et al., 2013; Hernandez et al., 2015; Oshkin et al., 2014). Compared to the complete oxidation of methane to CO₂, the Gibbs energies of partial oxidation reactions are ~6-fold (methanol) or 3- to 4-fold (formate, acetate) lower (Table 5). Higher contributions of energetically less favorable partial methane oxidation reactions in the eutrophic lakes could thus contribute to the lower MOB percentages in the latter. Yet, while we observe strong correlations between calculated *pmoA* copy numbers of certain Type I genus-level taxa and OTUs with calculated 16S gene copy numbers of Methylophilaceae (Figure 7B), the percentage of taxa or OTUs with such correlations does not change in relation to trophic state.

In conclusion, based on available data, enhanced oligochaete grazing is a plausible reason for the lower absolute abundances of MOB in eutrophic lakes, whereas the lower percentages of MOB in eutrophic lakes can be explained with enhanced methane ebullition and/or outcompetition of MOB for O₂ by aerobic organotrophs. By contrast, based on our correlation analyses, enhanced energy-sharing with syntrophic partner organisms is less likely to drive the lower percentages of MOB in eutrophic lakes.

Role of Respiration Zone in Structuring Major MOB Taxa

Analyses of *pmoA* genus-level taxa distributions indicate strong overlaps in community structure between different trophic states, and thus argue against the existence of distinct oligotrophic or eutrophic MOB taxa (Figure 5 & 6A). Instead, the highly significant correlation of sediment depth with taxon-level MOB community structure, combined with the clear taxon-specific differences in distributions relative to vertical respiration zones, point to respiration zone as a key driver of MOB community composition at the genus-level (Figure 5, 6A, and 7A).

Interestingly, the Type Ia genera *Methylobacter* and *Methylomonas* and Type Ib genus *Methylococcus*, and dominant OTUs within these genera, had their highest calculated average *pmoA* abundances in oxic sediments (Figure 7), even though at least members of *Methylobacter* and *Methylomonas* have been linked to facultative anaerobic metabolism with or without partner organisms (*Methylomonas*: NO₂⁻, NO₃⁻, ferrihydrite (Kits et al., 2015b, 2015a; Zheng et al., 2020)); *Methylobacter*: NO₃⁻ (Smith et al., 2018; van Grinsven et al., 2020a)). Other MOB, including the Unclassified Type Ia Methylococcaceae have peak *pmoA* abundances in suboxic layers (Figure 7), suggesting that members of this paraphyletic group might couple methane oxidation to nitrate reduction. Syntrophic interactions between unclassified Type Ia Methylococcaceae and *Methylomonas* and methylotrophic Methylophilaceae with denitrifying potential were previously proposed (Beck et al., 2013; Cao et al., 2019; van Grinsven et al., 2020b) and would match found correlations between *pmoA* abundances of both groups and 16S rRNA gene-based abundances of Methylophilaceae (Figure 7B).

While the observed distributions of Type I taxa are generally consistent with previous studies, the observed trends in Type II taxa are more difficult to reconcile. Type II alphaproteobacterial Methylocystaceae sequences dominated deep anoxic sediments of all lakes (Figure 6). It remains unclear whether these deep *Methylocystis*-related *pmoA* sequences derive from metabolically active cells, resting (dormant) or inactive cells, or dead organisms. For this DNA to be from dead cells, DNA of *Methylocystis* would need to be more effectively preserved than DNA of Type I methanotrophs, e.g. via shielding by more degradation-resistant cell walls. Members of *Methylocystis* produce lipoidal cysts as resting stages, which are compositionally distinct from the carbohydrate-rich (“*Azotobacter*-type”) cell walls of cysts produced by most Methylococcaceae (Bowman 2014). These lipoidal cysts may be more degradation-resistant in lake sediments than *Azotobacter*-type cysts. Yet, enhanced stability of resting stages, which requires substantiation, does not explain why dominant *Methylocystis*-related OTUs reach their highest gene copy numbers in anoxic layers where respiration is dominated by metal reduction and methanogenesis (Figure 7A), or why previous studies have reported increases in relative abundances and active assimilation of methane-C by Type II methanotrophs in anoxic sediment (Yang et al., 2019; He et al., 2012). A potential explanation is that Type II *Methylocystis*-related MOB oxidize methane *via* strictly anaerobic associations with partner organisms. Yet, only one *Methylocystis* OTU (out of 64) showed a significant correlation with a methylotrophic bacterial OTU (genus *Methyloceanibacteria*; Figure 7B and related text). Thus, deep Type II MOB might depend less on syntrophic interactions than their Type I counterparts in shallower layers, or not at all. Future research will reveal whether members of *Methylocystis* are involved in methane oxidation, e.g. coupled to metal reduction, as was previously shown for members of *Methylosinus*, a sister genus of *Methylocystis* (Zheng et al., 2020), or even subsist on substrates other than methane, such as acetate or ethanol as was previously shown for (however aerobic) members of this genus (Haque et al., 2020; Oshkin et al., 2020).

Lake Trophic State as a Driver of MOB Communities at the Species-Level

While *pmoA*-based community structure at the genus-level was similar across different trophic states, analyses at the OTU-level indicate trophic state as a major driver of MOB community structure at the species-level (Figure 6B). Sediments of the oligotrophic Lake Lucerne have a significantly lower OTU diversity and evenness than sediments of the meso- and eutrophic lakes (Figure 4) and are dominated by a small number of OTUs that are also present though not dominant in eu- and mesotrophic lakes (Supplementary Figure S2). Interestingly, as previously demonstrated for 16S rRNA gene-based analyses of bacterial communities (Han et al., 2020), the trophic state at the time of sediment deposition appears to better predict the present-day MOB community structure than the present-day trophic state of the lake in numerous cases. This

is indicated by the fact that OTU community fingerprints of several deep samples from Lake Zug and Lake Greifen, that were deposited under oligotrophic conditions, cluster with samples from the always oligotrophic Lake Lucerne (Figure 6B). This legacy effect was most evident in a Type Ib Methylococcaceae-related (OTU_2) and a Type II *Methylocystis*-related OTU (OTU_3). These OTUs dominated sediment samples from Lake Lucerne and had high relative abundances in deep oligotrophic samples from Lake Zug and Lake Greifen, while being nearly absent from all other samples (Supplementary Figure S2).

Our results indicate that MOB community structure is controlled by different environmental variables on different phylogenetic levels. The strong community structuring of MOB genus-level taxa in relation to respiration zones could reflect differences in electron acceptor use or methylo-trophic partners among these taxa. By contrast, the clear structuring of OTU-based communities relative to trophic state suggests that additional factors control MOB communities at the species or strain-level, such as differences in enzyme and transporter affinities in relation to nutrient regimes or competition with other microorganisms for O₂. The low community alpha-diversity and evenness in oligotrophic Lake Lucerne, where organic matter is more degraded and contains lower fractions of algal organic carbon, could reflect lower geochemical niche diversity, reduced availability of biosynthetic nutrients and reduced competition for O₂. In comparison, higher availability of nutrients needed for biomass production and higher diversity of microniches with distinct redox conditions could support higher numbers of co-existing OTUs and higher evenness in eutrophic lake sediments.

CONCLUSION

Although eutrophication is expected to increase lacustrine methane emissions worldwide, its effects on the methanotrophic and wider carbon-cycling microbial community are not well understood. Across five lakes in central Switzerland that range in present-day trophic state from highly eutrophic to oligotrophic, and differ significantly in trophic histories, we observe the highest *pmoA* copy numbers and contributions of MOB to total microbial communities under oligotrophic conditions. This observation is remarkable given the higher methane fluxes in the eutrophic lakes and considering that O₂ fluxes into sediments vastly exceed the amount required for complete mineralization of methane at most stations. Potential explanations include that most methane produced in eutrophic sediments “bypasses” MOB communities by ebullition into overlying water and/or that MOB are outcompeted for O₂ by organotrophic microorganisms with higher *in situ* energy yields in eutrophic lakes. In addition, microbial community size based on gene copy numbers may not represent a reliable proxy for MOB activity, suggesting that follow-up studies in which methanotrophic activity is measured are needed.

The consistent depth zonation of “aerobic” MOB in suboxic and anoxic sediments suggests that a much higher proportion

of MOB taxa is capable of anaerobic metabolism than previously assumed. The observed OTU-level community structuring according to trophic state at the time of sediment deposition, moreover, indicates a legacy effect of eutrophication on methanotrophic communities. Correlation analyses of MOB and potential methylo-trophic partner organisms suggest that syntrophic interactions between MOB and methylo-trophs are most important in oxic and denitrifying sediment, and less important in deeper layers where O₂ and nitrate are presumed to be absent. Future research will reveal whether Type II MOB that increase in deep, Fe-reducing and methanogenic layers engage in an unknown form of methanotrophy, and, if so, how methane oxidation is thermodynamically possible in the same sediment layers in which methane is also produced.

DATA AVAILABILITY STATEMENT

The datasets presented in this study can be found in online repositories. The names of the repository/repositories and accession number(s) can be found in the article/Supplementary Material.

AUTHOR CONTRIBUTIONS

ML designed the study. AM and XH performed the laboratory analyses. DM, SvG, ML, and CS analyzed the data. ML, SvG, and DM wrote the manuscript with input from all co-authors.

FUNDING

This study was funded by the Swiss National Science Foundation (project 205321_163371 “Role of bioturbation in controlling microbial community composition and biogeochemical cycles in marine and lacustrine sediments” awarded to ML).

ACKNOWLEDGMENTS

We thank Beat Müller (Eawag) for assistance with diffusive flux calculations, Nathalie Dubois, Alois Zwyssig, Alfred Lück, and Irene Brunner for sampling assistance (all Eawag), Annika Fiskal, Philip Eickenbusch, and Lorenzo Lagostina (all ETH Zurich) for technical support, and Silvia Kobel, Aria Minder, and Jean-Claude Walser from the Genetic Diversity Centre (GDC; ETH Zurich) for assistance with next-generation sequencing and bioinformatic analyses.

SUPPLEMENTARY MATERIAL

The Supplementary Material for this article can be found online at: <https://www.frontiersin.org/articles/10.3389/fenvs.2022.857358/full#supplementary-material>

REFERENCES

- Anderson, N. J., Bennion, H., and Lotter, A. F. (2014). Lake Eutrophication and its Implications for Organic Carbon Sequestration in Europe. *Glob. Change Biol.* 20, 2741–2751. doi:10.1111/gcb.12584
- Auman, A. J., Stolyar, S., Costello, A. M., and Lidstrom, M. E. (2000). Molecular Characterization of Methanotrophic Isolates from Freshwater Lake Sediment. *Appl. Environ. Microbiol.* 66, 5259–5266. doi:10.1128/aem.66.12.5259-5266.2000
- Bastviken, D., Cole, J. J., Pace, M. L., and van de Bogert, M. C. (2008). Fates of Methane from Different Lake Habitats: Connecting Whole-lake Budgets and CH₄ Emissions. *J. Geophys. Res.* 113, a–n. doi:10.1029/2007JG000608
- Bastviken, D., Cole, J., Pace, M., and Tranvik, L. (2004). Methane Emissions from Lakes: Dependence of Lake Characteristics, Two Regional Assessments, and a Global Estimate. *Glob. Biogeochem. Cycles* 18, a–n. doi:10.1029/2004GB002238
- Bastviken, D., Tranvik, L. J., Downing, J. A., Crill, P. M., and Enrich-Prast, A. (2011). Freshwater Methane Emissions Offset the Continental Carbon Sink. *Science* 331, 50. doi:10.1126/science.1196808
- Beals, E. W. (1984). Bray-curtis Ordination: An Effective Strategy for Analysis of Multivariate Ecological Data. *Adv. Ecol. Res.* 14, 1–55. doi:10.1016/S0065-2504(08)60168-3
- Beaulieu, J. J., DelSontro, T., and Downing, J. A. (2019). Eutrophication Will Increase Methane Emissions from Lakes and Impoundments during the 21st century. *Nat. Commun.* 10, 3–7. doi:10.1038/s41467-019-09100-5
- Beck, D. A. C., Kalyuzhnaya, M. G., Malfatti, S., Tringe, S. G., Glavina del Rio, T., Ivanova, N., et al. (2013). A Metagenomic Insight into Freshwater Methane-Utilizing Communities and Evidence for Cooperation between the Methylococcales and the Methylophilaceae. *PeerJ* 1, e23. doi:10.7717/peerj.23
- Bowman, J. P. (2014). The Family Methylococcales. *The Prokaryotes: Gammaproteobacteria* 9783642389, 411–440. doi:10.1007/978-3-642-38922-1_237
- Buergi, H. R., and Stadelmann, R. (2000). für, R. S.-I. V., and 2000, undefined Change of phytoplankton diversity during long-term restoration of Lake Baldeggen (Switzerland). *SIL Proc. 1922-2010* 27, 574–581. doi:10.1080/03680770.1998.11901300
- Cao, Q., Liu, X., Ran, Y., Li, Z., and Li, D. (2019). Methane Oxidation Coupled to Denitrification under Microaerobic and Hypoxic Conditions in Leach Bed Bioreactors. *Sci. Total Environ.* 649, 1–11. doi:10.1016/j.scitotenv.2018.08.289
- Chen, I.-M. A., Chu, K., Palaniappan, K., Ratner, A., Huang, J., Huntemann, M., et al. (2021). The IMG/M Data Management and Analysis System v.6.0: New Tools and Advanced Capabilities. *Nucleic Acids Res.* 49, D751–D763. doi:10.1093/NAR/GKAA939
- Chen, J., He, F., Zhang, X., Sun, X., Zheng, J., and Zheng, J. (2014). Heavy Metal Pollution Decreases Microbial Abundance, Diversity and Activity within Particle-Size Fractions of a Paddy Soil. *FEMS Microbiol. Ecol.* 87, 164–181. doi:10.1111/1574-6941.12212
- Costello, A. M., and Lidstrom, M. E. (1999). Molecular Characterization of Functional and Phylogenetic Genes from Natural Populations of Methanotrophs in Lake Sediments. *Appl. Environ. Microbiol.* 65, 5066–5074. doi:10.1128/aem.65.11.5066-5074.1999
- D'Ambrosio, S., and Harrison, J. A. (2021). Methanogenesis Exceeds CH₄ Consumption in Eutrophic Lake Sediments. *Limnol. Oceanogr. Lett.* 6, 173–181. doi:10.1002/lol2.10192
- Danilova, O. V., Suzina, N. E., Van De Kamp, J., Svenning, M. M., Bodrossy, L., and Dedysh, S. N. (2016). A New Cell Morphotype Among Methane Oxidizers: A Spiral-Shaped Obligately Microaerophilic Methanotroph from Northern Low-Oxygen Environments. *ISME J.* 10, 2734–2743. doi:10.1038/ismej.2016.48
- Dean, J. F., Middelburg, J. J., Röckmann, T., Aerts, R., Blauw, L. G., Egger, M., et al. (2018). Methane Feedbacks to the Global Climate System in a Warmer World. *Rev. Geophys.* 56, 207–250. doi:10.1002/2017RG000559
- Deines, P., Bodelier, P. L., and Eller, G. (2007). Methane-derived Carbon Flows through Methane-Oxidizing Bacteria to Higher Trophic Levels in Aquatic Systems. *Environ. Microbiol.* 9, 1126–1134. doi:10.1111/j.1462-2920.2006.01235.x
- Deutzmann, J. S., Stief, P., Brandes, J., and Schink, B. (2014). Anaerobic Methane Oxidation Coupled to Denitrification Is the Dominant Methane Sink in a Deep lake. *Proc. Natl. Acad. Sci. USA* 111, 18273–18278. doi:10.1073/pnas.1411617111
- de Valk, S., Khadem, A. F., Foreman, C. M., van Lier, J. B., and de Kreuk, M. K. (2017). Physical and Biochemical Changes in Sludge Upon Tubifex Tubifex Predation. *Environ. Technol.* 38, 1524–1538. doi:10.1080/09593330.2016.1236150
- Di Cesare, A., Pjevac, P., Eckert, E., Curkov, N., Miko Šparica, M., Corno, G., et al. (2020). The Role of Metal Contamination in Shaping Microbial Communities in Heavily Polluted Marine Sediments. *Environ. Pollut.* 265, 114823. doi:10.1016/j.envpol.2020.114823
- Ettwig, K. F., Butler, M. K., Le Paslier, D., Pelletier, E., Mangenot, S., Kuypers, M. M., et al. (2010). Nitrite-driven Anaerobic Methane Oxidation by Oxygenic Bacteria. *Nature* 464, 543–548. doi:10.1038/nature08883
- Ettwig, K. F., Zhu, B., Speth, D., Keltjens, J. T., Jetten, M. S. M., and Kartal, B. (2016). Archaea Catalyze Iron-dependent Anaerobic Oxidation of Methane. *Proc. Natl. Acad. Sci. USA* 113, 12792–12796. doi:10.1073/pnas.1609534113
- Farhan Ul Haque, M., Xu, H.-J., Murrell, J. C., and Crombie, A. (2020). Facultative Methanotrophs - Diversity, Genetics, Molecular Ecology and Biotechnological Potential: a Mini-Review. *Microbiol. (United Kingdom)* 166, 894–908. doi:10.1099/mic.0.000977
- Fiskal, A., Anthamatten, E., Deng, L., Han, X., Lagostina, L., Michel, A., et al. (2021a). Carbon Sources of Benthic Fauna in Temperate Lakes across Multiple Trophic States. *Biogeosciences* 18, 4369–4388. doi:10.5194/bg-18-4369-2021
- Fiskal, A., Gaillard, A., Giroud, S., Malcic, D., Joshi, P., Sander, M., et al. (2021b). Effects of Macrofaunal Recolonization on Biogeochemical Processes and Microbiota a Mesocosm Study. *Water* 13, 1599. doi:10.3390/w13111599
- Fiskal, A., Deng, L., Michel, A., Eickenbusch, P., Han, X., Lagostina, L., et al. (2019). Effects of Eutrophication on Sedimentary Organic Carbon Cycling in Five Temperate Lakes. *Biogeosciences* 16, 3725–3746. doi:10.5194/bg-16-3725-2019
- Frenzel, P., Thebrath, B., and Conrad, R. (1990). Oxidation of Methane in the Oxidic Surface Layer of a Deep Lake Sediment (Lake Constance). *FEMS Microbiol. Lett.* 73, 149–158. doi:10.1016/0378-1097(90)90661-910.1111/j.1574-6968.1990.tb03935.x
- Grinsven, S., Sinnighe Damsté, J. S., Engelmann, J. C., Harrison, J., Villanueva, L., and Villanueva, L. (2020a). Methane Oxidation in Anoxic Lake Water Stimulated by Nitrate and Sulfate Addition. *Environ. Microbiol.* 22, 766–782. doi:10.1111/1462-2920.14886
- Grinsven, S., Sinnighe Damsté, J. S., Polerecky, L., Villanueva, L., and Villanueva, L. (2020b). Nitrate Promotes the Transfer of Methane-derived Carbon from the Methanotroph *Methylobacter* Sp. to the Methylophilic *Methylothermus* Sp. in Eutrophic Lake Water. *Limnol. Oceanogr.* 66, 878–891. doi:10.1002/lno.11648
- Guo, M., Zhuang, Q., Tan, Z., Shurpali, N., Juutinen, S., Kortelainen, P., et al. (2020). Rising Methane Emissions from Boreal Lakes Due to Increasing Ice-free Days. *Environ. Res. Lett.* 15, 064008. doi:10.1088/1748-9326/ab8254
- Han, X., Schubert, C. J., Fiskal, A., Dubois, N., and Lever, M. A. (2020). Eutrophication as a Driver of Microbial Community Structure in Lake Sediments. *Environ. Microbiol.* 22, 3446–3462. doi:10.1111/1462-2920.15115
- He, R., Wooller, M. J., Pohlman, J. W., Quensen, J., Tiedje, J. M., and Leigh, M. B. (2012). Shifts in Identity and Activity of Methanotrophs in Arctic Lake Sediments in Response to Temperature Changes. *Appl. Environ. Microbiol.* 78, 4715–4723. doi:10.1128/AEM.00853-12
- He, R., Wang, J., Pohlman, J. W., Jia, Z., Chu, Y.-X., Wooller, M. J., et al. (2021). Metabolic Flexibility of Aerobic Methanotrophs under Anoxic Conditions in Arctic Lake Sediments. *ISME J.* 16, 78–90. doi:10.1038/s41396-021-01049-y
- Heathcote, A. J., and Downing, J. A. (2012). Impacts of Eutrophication on Carbon Burial in Freshwater Lakes in an Intensively Agricultural Landscape. *Ecosystems* 15, 60–70. doi:10.1007/s10021-011-9488-9
- Hernandez, M. E., Beck, D. A. C., Lidstrom, M. E., and Chistoserdova, L. (2015). Oxygen Availability is a Major Factor in Determining the Composition of Microbial Communities Involved in Methane Oxidation. *Peer J* 3, e801. doi:10.7717/peerj.801
- Holmes, A. J., Costello, A., Lidstrom, M. E., and Murrell, J. C. (1995). Evidence that Participate Methane Monooxygenase and Ammonia Monooxygenase May Be Evolutionarily Related. *FEMS Microbiol. Lett.* 132, 203–208. doi:10.1111/j.1574-6968.1995.tb07834.x
- Jones, R. I., and Grey, J. (2011). Biogenic Methane in Freshwater Food Webs. *Freshw. Biol.* 56, 213–229. doi:10.1111/j.1365-2427.2010.02494.x

- Kalyuzhnaya, M. G., Yang, S., Rozova, O. N., Smalley, N. E., Clubb, J., Lamb, A., et al. (2013). Highly Efficient Methane Biocatalysis Revealed in a Methanotrophic Bacterium. *Nat. Commun.* 4, 1–7. doi:10.1038/ncomms3785
- Kits, K. D., Campbell, D. J., Rosana, A. R., and Stein, L. Y. (2015a). Diverse Electron Sources Support Denitrification under Hypoxia in the Obligate Methanotroph *Methylobacterium Album* Strain BG8. *Front. Microbiol.* 6, 1–11. doi:10.3389/fmicb.2015.01072
- Kits, K. D., Klotz, M. G., and Stein, L. Y. (2015b). Methane Oxidation Coupled to Nitrate Reduction under Hypoxia by the Gammaproteobacterium *Methylobacterium Album* Strain FJG1. *Environ. Microbiol.* 17, 3219–3232. doi:10.1111/1462-2920.12772
- Kiyashko, S., Narita, T., and Wada, E. (2001). Contribution of Methanotrophs to Freshwater Macroinvertebrates: Evidence from Stable Isotope Ratios. *Aquat. Microb. Ecol.* 24, 203–207. doi:10.3354/ame024203
- Knief, C. (2015). Diversity and Habitat Preferences of Cultivated and Uncultivated Aerobic Methanotrophic Bacteria Evaluated Based on *pmoA* as Molecular Marker. *Front. Microbiol.* 6, 1346. doi:10.3389/fmicb.2015.01346
- Lennartz, S. (2010). Zinn in Den Sedimenten Des Zürichsees. PhD thesis. Germany: Univ. of Tübingen.
- Lerman, A. (1979). *Geochemical Processes: Water and Sediment Environments*. New York, NY: John Wiley & Sons.
- Leu, A. O., Cai, C., McIlroy, S. J., Southam, G., Orphan, V. J., Yuan, Z., et al. (2020). Anaerobic Methane Oxidation Coupled to Manganese Reduction by Members of the Methanoperedenaceae. *ISME J.* 14, 1030–1041. doi:10.1038/s41396-020-0590-x
- Lever, M. A., Torti, A., Eickenbusch, P., Michaud, A. B., Säntl-Temkiv, T., Jørgensen, B. B., et al. (2015). A Modular Method for the Extraction of DNA and RNA, and the Separation of DNA Pools from Diverse Environmental Sample Types. *Front. Microbiol.* 6, 476. doi:10.3389/fmicb.2015.00476
- Lloréns-Rico, V., Vieira-Silva, S., Gonçalves, P. J., Falony, G., and Raes, J. (2021). Benchmarking Microbiome Transformations Favors Experimental Quantitative Approaches to Address Compositionality and Sampling Depth Biases. *Nat. Commun.* 12. doi:10.1038/s41467-021-23821-6
- Ludwig, W., Strunk, O., Westram, R., Richter, L., Meier, H., Yadukumar, A., et al. (2004). ARB: A Software Environment for Sequence Data. *Nucleic Acids Res.* 32, 1363–1371. doi:10.1093/nar/gkh293
- Lyautey, E., Billard, E., Tissot, N., Jacquet, S., and Domaizon, I. (2021). Seasonal Dynamics of Abundance, Structure, and Diversity of Methanogens and Methanotrophs in Lake Sediments. *Microb. Ecol.* 82, 559–571. doi:10.1007/s00248-021-01689-9
- Maerki, M., Wehrli, B., Dinkel, C., and Müller, B. (2004). The Influence of Tortuosity on Molecular Diffusion in Freshwater Sediments of High Porosity 1 Associate Editor: M. L. Machesky. *Geochimica et Cosmochimica Acta* 68, 1519–1528. doi:10.1016/j.gca.2003.09.019
- Mayr, M. J., Zimmermann, M., Guggenheim, C., Brand, A., and Bürgmann, H. (2020). Niche Partitioning of Methane-Oxidizing Bacteria along the Oxygen-Methane Counter Gradient of Stratified Lakes. *ISME J.* 14, 274–287. doi:10.1038/s41396-019-0515-8
- McDonald, I. R., Bodrossy, L., Chen, Y., and Murrell, J. C. (2008). Molecular Ecology Techniques for the Study of Aerobic Methanotrophs. *Appl. Environ. Microbiol.* 74, 1305–1315. doi:10.1128/AEM.02233-07
- Mukherjee, S., Stamatis, D., Bertsch, J., Ovchinnikova, G., Sundaramurthi, J. C., Lee, J., et al. (2021). Genomes OnLine Database (GOLD) v.8: Overview and Updates. *Nucleic Acids Res.* 49, D723–D733. doi:10.1093/nar/gkaa983
- Müller, B., Wang, Y., Dittrich, M., and Wehrli, B. (2003). Influence of Organic Carbon Decomposition on Calcite Dissolution in Surficial Sediments of a Freshwater Lake. *Water Res.* 37, 4524–4532. doi:10.1016/S0043-1354(03)00381-6
- Naeher, S., Gilli, A., North, R. P., Hamann, Y., and Schubert, C. J. (2013). Tracing Bottom Water Oxygenation with Sedimentary Mn/Fe Ratios in Lake Zurich, Switzerland. *Chem. Geology.* 352, 125–133. doi:10.1016/j.chemgeo.2013.06.006
- Ogle, D., Doll, J., Wheeler, P., and Dinno, A. (2021). FSA: Fisheries Stock Analysis. R package version 0.9.1, Available at: <https://github.com/droglenc/FSA>.
- Oksanen, J., Blanchet, F. G., Friendly, M., Kindt, R., Legendre, P., and McGlenn, D. (2020). Vegan: Community Ecology Package: R Package Version 2.5-7. Available at: [https://scholar.google.com/scholar?hl=en&as_sdt=0%2C5&q=vegan%3A+Community+Ecology+Package.+R+++package+version+2.5-7&btnG=\[Accessed January 11, 2022\]](https://scholar.google.com/scholar?hl=en&as_sdt=0%2C5&q=vegan%3A+Community+Ecology+Package.+R+++package+version+2.5-7&btnG=[Accessed+January+11,+2022]).
- Oshkin, I. Y., Beck, D. A., Lamb, A. E., Tchesnokova, V., Benuska, G., McTaggart, T. L., et al. (2014). Methane-fed Microbial Microcosms Show Differential Community Dynamics and Pinpoint Taxa Involved in Communal Response. *ISME J.* 9, 1119–1129. doi:10.1038/ismej.2014.203
- Oshkin, I. Y., Miroshnikov, K. K., Grouzdev, D. S., and Dedysh, S. N. (2020). Pan-genome-based Analysis as a Framework for Demarcating Two Closely Related Methanotroph Genera *Methylocystis* and *Methylosinus*. *Microorganisms* 8, 768. doi:10.3390/microorganisms8050768
- Oswald, K., Milucka, J., Brand, A., Hach, P., Littmann, S., Wehrli, B., et al. (2016). Aerobic Gammaproteobacterial Methanotrophs Mitigate Methane Emissions from Oxidic and Anoxic Lake Waters. *Limnol. Oceanogr.* 61, S101–S118. doi:10.1002/lno.10312
- Pester, M., Schleper, C., and Wagner, M. (2011). The Thaumarchaeota: an Emerging View of Their Phylogeny and Ecophysiology. *Curr. Opin. Microbiol.* 14, 300–306. doi:10.1016/j.mib.2011.04.007
- Pierangeli, G. M. F., Domingues, M. R., Jesus, T. A. d., Coelho, W. S., Pompêo, M. L. M., Saia, F. T., et al. (2021). Higher Abundance of Sediment Methanogens and Methanotrophs Do Not Predict the Atmospheric Methane and Carbon Dioxide Flows in Eutrophic Tropical Freshwater Reservoirs. *Front. Microbiol.* 12, 1–15. doi:10.3389/fmicb.2021.647921
- Rahalkar, M., Deutzmann, J., Schink, B., and Bussmann, I. (2009). Abundance and Activity of Methanotrophic Bacteria in Littoral and Profundal Sediments of Lake Constance (Germany). *Appl. Environ. Microbiol.* 75, 119–126. doi:10.1128/AEM.01350-08
- Reim, A., Lücke, C., Krause, S., Pratscher, J., and Frenzel, P. (2012). One Millimetre Makes the Difference: High-Resolution Analysis of Methane-Oxidizing Bacteria and Their Specific Activity at the Oxidic-Anoxic Interface in a Flooded Paddy Soil. *ISME J.* 6, 2128–2139. doi:10.1038/ismej.2012.57
- Rognes, T., Flouri, T., Nichols, B., Quince, C., and Mahé, F. (2016). VSEARCH: A Versatile Open Source Tool for Metagenomics. *PeerJ* 4, e2584. doi:10.7717/PEERJ.2584/FIG-7
- Sanches, L. F., Guenet, B., Marinho, C. C., Barros, N., and de Assis Esteves, F. (2019). Global Regulation of Methane Emission from Natural Lakes. *Sci. Rep.* 9, 1–10. doi:10.1038/s41598-018-36519-5
- Schubert, C. J., Diem, T., and Eugster, W. (2012). Methane Emissions from a Small Wind Shielded Lake Determined by Eddy Covariance, Flux Chambers, Anchored Flux Towers, and Boundary Model Calculations: A Comparison. *Environ. Sci. Technol.* 46, 4515–4522. doi:10.1021/es203465x
- Smith, G. J., Angle, J. C., Solden, L. M., Borton, M. A., Morin, T. H., Daly, R. A., et al. (2018). Members of the Genus *Methylobacter* Are Inferred to Account for the Majority of Aerobic Methane Oxidation in Oxidic Soils from a Freshwater Wetland. *MBio* 9, 1–17. doi:10.1128/mBio.00815-18
- Teranes, J. L., McKenzie, J. A., Lotter, A. F., and Sturm, M. (1999). Stable Isotope Response to Lake Eutrophication: Calibration of a High-Resolution Lacustrine Sequence from Baldeggersee, Switzerland. *Limnol. Oceanogr.* 44, 320–333. doi:10.4319/lno.1999.44.2.0320
- Thauer, R. K., Jungermann, K., and Decker, K. (1977). Energy Conservation in Chemotrophic Anaerobic Bacteria. *Bacteriol. Rev.* 41, 100–180. doi:10.1128/br.41.1.100-180.1977
- Thebrath, B., Rothfuss, F., Whiticar, M. J., and Conrad, R. (1993). Methane Production in Littoral Sediment of Lake Constance. *FEMS Microbiol. Ecol.* 102, 279–289. doi:10.1111/j.1574-6968.1993.tb05819.x
- Thottathil, S. D., Reis, P. C. J., del Giorgio, P. A., and Prairie, Y. T. (2018). The Extent and Regulation of Summer Methane Oxidation in Northern Lakes. *J. Geophys. Res. Biogeosci.* 123, 3216–3230. doi:10.1029/2018JG004464
- Tranvik, L. J., Downing, J. A., Cotner, J. B., Loiselle, S. A., Striegl, R. G., Ballatore, T. J., et al. (2009). Lakes and Reservoirs as Regulators of Carbon Cycling and Climate. *Limnol. Oceanogr.* 54, 2298–2314. doi:10.4319/lno.2009.54.6_part_2.2298
- Tsutsumi, M., Kojima, H., and Fukui, M. (2012). Vertical Profiles of Abundance and Potential Activity of Methane-Oxidizing Bacteria in Sediment of Lake Biwa, Japan. *Microb. Environ.* 27, 67–71. doi:10.1264/jsme2.ME11285
- van Grinsven, S., Oswald, K., Wehrli, B., Jegge, C., Zopfi, J., Lehmann, M. F., et al. (2021). Methane Oxidation in the Waters of a Humic-Rich Boreal Lake Stimulated by Photosynthesis, Nitrite, Fe(III) and Humics. *Biogeochemistry* 18, 3087–3101. doi:10.5194/bg-18-3087-2021
- Vekeman, B., Kerckhof, F.-M., Cremers, G., de Vos, P., Vandamme, P., Boon, N., et al. (2016). New *Methyloceanibacter* Diversity from North Sea Sediments Includes

- Methanotroph Containing Solely the Soluble Methane Monooxygenase. *Environ. Microbiol.* 18, 4523–4536. doi:10.1111/1462-2920.13485
- Wickham, H. (2016). *ggplot2: Elegant Graphics for Data Analysis*. New York, NY: Springer-Verlag.
- Yang, Y., Chen, J., Tong, T., Li, B., He, T., Liu, Y., et al. (2019). Eutrophication Influences Methanotrophic Activity, Abundance and Community Structure in Freshwater Lakes. *Sci. Total Environ.* 662, 863–872. doi:10.1016/j.scitotenv.2019.01.307
- Yang, Y., Zhao, Q., Cui, Y., Wang, Y., Xie, S., and Liu, Y. (2016). Spatio-temporal Variation of Sediment Methanotrophic Microorganisms in a Large Eutrophic lake. *Microb. Ecol.* 71, 9–17. doi:10.1007/s00248-015-0667-7
- Zheng, Y., Wang, H., Liu, Y., Zhu, B., Li, J., Yang, Y., et al. (2020). Methane-Dependent Mineral Reduction by Aerobic Methanotrophs under Hypoxia. *Environ. Sci. Technol. Lett.* 7, 606–612. doi:10.1021/acs.estlett.0c00436
- Zhu, Y., Purdy, K. J., Eyice, Ö., Shen, L., Harpenslager, S. F., Yvon-Durocher, G., et al. (2020). Disproportionate Increase in Freshwater Methane Emissions Induced by Experimental Warming. *Nat. Clim. Chang.* 10, 685–690. doi:10.1038/s41558-020-0824-y

Conflict of Interest: The authors declare that the research was conducted in the absence of any commercial or financial relationships that could be construed as a potential conflict of interest.

Publisher's Note: All claims expressed in this article are solely those of the authors and do not necessarily represent those of their affiliated organizations, or those of the publisher, the editors and the reviewers. Any product that may be evaluated in this article, or claim that may be made by its manufacturer, is not guaranteed or endorsed by the publisher.

Copyright © 2022 van Grinsven, Meier, Michel, Han, Schubert and Lever. This is an open-access article distributed under the terms of the Creative Commons Attribution License (CC BY). The use, distribution or reproduction in other forums is permitted, provided the original author(s) and the copyright owner(s) are credited and that the original publication in this journal is cited, in accordance with accepted academic practice. No use, distribution or reproduction is permitted which does not comply with these terms.